Title page

Title:

Notch4 reveals a novel mechanism regulating Notch signal transduction

Running title:

Notch4 inhibits Notch1 signalling

James, A.C.[a], Szot, J.O.[a,c], Iyer, K.[a], Major, J.A.[a], Pursglove, S.E.[a], Chapman, G.[a,b,#], Dunwoodie, S.L.[a,b,c,#,*]

a. Developmental and Stem Cell Biology Division, Victor Chang Cardiac Research Institute, Sydney, Australia

b. St Vincent's Clinical School, Faculty of Medicine, UNSW, Sydney, Australia

c. School of Biotechnology and Biomolecular Sciences, Faculty of Science, UNSW, Sydney, Australia

joint authors.

* corresponding author: 405 Liverpool Street, Darlinghurst, NSW, 2010, Australia. Tel: +612 9295 8613

Author email addresses:

ACJ: a.james@victorchang.edu.au

JOS: j.szot@victorchang.edu.au

KI: k.iyer@victorchang.edu.au

JAM: j.major@victorchang.edu.au

SEP: sharonchapman2201@gmail.com

GC: g.chapman@victorchang.edu.au

SLD: s.dunwoodie@victorchang.edu.au

Abstract

Notch4 is a divergent member of the Notch family of receptors that is primarily expressed in the vasculature. Its expression implies an important role for *Notch4* in the vasculature; however, mice homozygous for the *Notch4*^{d1} knockout allele are viable. Since little is known about the role of *Notch4* in the vasculature and how it functions, we further investigated Notch4 in mice and in cultured cells. We and found that the *Notch4*^{d1} allele is not null as it expresses a truncated transcript encoding most of the NOTCH4 extracellular domain. In cultured cells, NOTCH4 did not signal in response to ligand. Moreover, NOTCH4 inhibited signalling from the NOTCH1 receptor. This is the first report of *cis*-inhibition of signalling by another Notch receptor. The NOTCH4 extracellular domain also inhibits NOTCH1 signalling when expressed *in cis*, raising the possibility that reported *Notch4* phenotypes may not be due to loss of NOTCH4 function. To better address the role of NOTCH4 *in vivo*, we generated a *Notch4* null mouse in which the entire coding region was deleted. *Notch4* null mice exhibited slightly delayed vessel growth in the retina, consistent with our novel finding that NOTCH4 protein is expressed in the newly formed vasculature. These findings indicate a role of NOTCH4 in fine-tuning the forming vascular plexus.

Keywords

Notch4, retinal angiogenesis, *cis*-inhibition, coculture

1. Introduction

Angiogenesis, the formation of new blood vessels from existing vasculature, is critical to the creation of an efficient vascular system. While angiogenesis does not take place in most adult tissues, it is an essential aspect of the wound healing response and recovery following ischemia to reoxygenate and supply nutrients to affected sites. Angiogenesis also contributes to pathologies such as tumour growth and metastasis, ocular and autoimmune diseases [1]. Moreover, a lack of appropriate angiogenesis can cause heart and brain ischemia, neurodegeneration, and preeclampsia [2]. Thus, proper control of angiogenesis in the embryo and adult is essential to generate a functioning vasculature and also to avoid pathology.

A number of signalling pathways including the Notch pathway are essential for angiogenesis. Notch signalling is necessary for laying down the primary vascular plexus and subsequently for arterial specification [3], vessel size and maturation [4,5] and for arteriogenesis in response to ischemia [6-9]. The roles of Notch receptors and ligands in angiogenesis have been elucidated in embryogenesis. The absence of the *Notch1* receptor or ligands *Jagged1 (Jag1)*, *Delta-like 1* (*Dll1)* or *Delta-like 4 (Dll4)* causes embryonic death from disrupted angiogenesis [3,10-12]. The NOTCH1 receptor is the most important Notch receptor in terms of its role in the vasculature. *Notch1* is widely expressed in the embryo generally as well as in the vasculature [13] and in its absence embryos die at embryonic day (E) 9.5 with reduced and abnormal angiogenesis of the embryo, yolk sac and placenta [11,14]. The most potent ligand of Notch with respect to angiogenesis is DLL4. Loss of even one copy of *Dll4* results in embryonic lethality with extensive angiogenic defects including pericardial edema, aortic atresia, and loss of the internal carotid artery and yolk sac vessels [10,15]. Notch signalling is important for both sprouting and intussusceptive (or splitting) angiogenesis [16-19]. During sprouting angiogenesis, tips cells arise at the leading edge of the expanding vascular plexus. These tip cells prevent neighbouring vascular endothelial cells from adopting the same fate through the Notch-dependent processes of lateral induction and lateral inhibition [20]. Tip cells at the leading edge of the vascular plexus express *Dll4* in response to VEGF and DLL1 in surrounding tissue [21,22]. DLL4 in tip cells is likely to induce Notch signal transduction in adjacent cells and thereby suppress the tip cell phenotype in these adjacent stalk cells [17]. Notch signalling, by limiting tip cell formation at the edge of the vascular plexus,

---

Abbreviations: ANK, Ankyrin repeat; DSL, Delta, Serrate and Lag-2; JAG1, Jagged1; DLL1, Delta-like 1; DLL4, Delta-like 4; E, Embryonic day; EC, extracellular domain; EGF, Epidermal Growth Factor; ER, Endoplasmic Reticulum; ES, Embryonic Stem; HD, Heterodimerisation Domain; IB4, Isolectin B4; ICD, Notch Intracellular Domain; NA, LNR, Lin12-Notch Repeat; Numerical Aperture; MAEC, Mouse Aortic Endothelial Cells; P, Postnatal day; PEST, Proline, Glutamate, Serine, and Tyrosine; RACE, Rapid Amplification of cDNA Ends; RAVE, Rapid Analysis of Vessel Elements; TAD, transcriptional activation domain; TGN, *trans*-Golgi Network

controls the extent of vessel branching. Accordingly, reduced levels of DLL4-Notch signalling disrupts sprouting angiogenesis due to overproduction of tip cells [17-19].

The Notch signal transduction pathway is critical for many aspects of embryonic development and homeostasis in the adult. Canonical Notch signalling occurs in a juxtacrine manner as Notch receptors and Delta, Serrate, Lag-2 (DSL) family ligands are transmembrane proteins. Signalling relies on post-translational modification of Notch, its presentation on the cell surface and receptor cleavage; these processes have largely been identified through the study of *Drosophila* Notch and mammalian NOTCH1 and NOTCH2. Mammalian Notch receptors are synthesised as a single polypeptide and undergo S1-cleavage in the *trans*-Golgi network (TGN) by Furin or a Furin-like convertase [23,24]. A heterodimer is formed by noncovalent linkage of the extracellular domain with the transmembrane and intracellular domains. Heterodimeric Notch is then transported to the cell surface where it can interact with ligands of the DSL family as well with other families of ligands, on neighbouring cells (*trans* interaction) [23,24]. In the case of NOTCH1, surface presentation of heterodimer is required for potent signal transduction [25]. Interaction between ligand and receptor *in trans* results in proteolytic cleavage (S2-cleavage) of Notch by ADAM10 [26-28]. The γ-secretase complex subsequently cleaves S2-cleaved Notch within the membrane (S3-cleavage), releasing the Notch intracellular domain (ICD) [29,30]. The ICD translocates to the nucleus and forms a complex with the DNA-binding protein CSL and MAML proteins. Direct targets of Notch include members of the hairy/enhancer-of-split (HES) and HES-related (HEY) family of bHLH transcription factors, Nrarp, and Lfng [31-34].

Of the four mammalian Notch receptors, signalling via NOTCH1 and NOTCH2 is best understood and it is assumed that NOTCH3 and NOTCH4 signal in a similar manner, as the ICD of each receptor interacts with CSL and transactivates Notch target genes [32,35,36]. In particular, *Notch4* is the most divergent of the four mammalian Notch receptors and is distinct as it is expressed almost exclusively in the vasculature, compared to *Notch1*, which is expressed in virtually all tissue types in the developing embryo [37]. In cultured cells, NOTCH4 is reported to signal in response to ligand [38,39] but little else is known about its mechanism of signal transduction. Studies in mice show that endothelial specific expression of constitutively active NOTCH4 (encoded by the *int3* allele) causes dramatic vascular changes including lack of small branched vessels, loss of vessel integrity [40,41] and arterial shunts [42,43]. Induction of *int3* expression in mature vessel endothelium (postnatally), causes expression of the Notch target gene *EphrinB2* and increased smooth muscle layers, resulting in arterialisation of venous vessels [40]. Such findings, coupled with the endothelial specific expression pattern of NOTCH4, imply that upon activation NOTCH4 would illicit similar effects on the vasculature and in so doing function to control the growth and differentiation of endothelial cells *in vivo*. However, this does not appear to

be the case as mice homozygous for the *Notch4* knockout allele (*Notch4*^{d1}) are viable [11]. *Notch4*^{d1} interacts with a *Notch1* null allele as about half of the embryos homozygous for both *Notch4*^{d1} and *Notch1* null are more severely affected than *Notch1* null embryos [11]. These defects include open neural tubes, fewer somites and collapse of the anterior cardinal vein [11]. Adult mice homozygous for the *Notch4*^{d1} allele exhibit slightly elevated blood pressure [9], delayed tumour onset and reduced tumour perfusion [44]. Since *Notch4* and *Notch1* are expressed in the vasculature, it is considered that *Notch1* compensates for the loss of *Notch4* [13,37,45-47].

Currently our understanding of the role of *Notch4* in the vasculature is not clear. Therefore we further examined the *Notch4*^{d1} allele in mice, and the signalling potential of the wildtype NOTCH4 receptor in cultured cells. We report that the *Notch4* knockout allele *Notch4*^{d1}, expresses a truncated transcript encoding most of the extracellular domain of the receptor. Moreover, in cultured cells we find that NOTCH4, unlike the other Notch receptors, lacks detectable signalling capacity and instead inhibits signalling from NOTCH1 when both receptors are expressed in the same cells. Importantly, the truncated NOTCH4d1 receptor expressed by *Notch4*^{d1} mice retains the capacity to inhibit NOTCH1 signalling *in cis*; it is therefore not a *Notch4* null allele. To determine the effect of a complete loss of *Notch4*, we generated mice lacking the entire *Notch4* coding region. These *Notch4* null mice are viable but they exhibit a delayed growth in retinal angiogenesis, pointing to a subtle role for NOTCH4 in developmental angiogenesis.

2. Materials and Methods

2.1. Mice

Notch4^{tm1Grid}, referred to as *Notch4*^{d1}, was a kind gift from Thomas Gridley [11]. A mouse line, *Notch4*$^{tm1(KOMP)Vlcg}$ referred to as *Notch4*$^{-}$, carrying a deletion allele of *Notch4* was made by the Australian Phenomics Network using embryonic stem cells obtained from the KOMP repository (project number 10800). Gene targeting of the insertion cassette (Zen-Ub-1), containing the neomycin resistance gene and a LacZ reporter, replaced the entire open reading frame of *Notch4* (bases 34,724,940—34,701,394 of chromosome 17). The resulting mice were housed at the Biocore, Victor Chang Cardiac Research Institute and kept in a perpetual 12 hour light/dark cycle and fed *ad libitum*.

Notch4$^{+/-}$ males and females were paired for timed matings in the afternoon and plugs checked the following morning. Pairings were left for 3 days before separation or identification of a vaginal plug. Plug date was considered 0.5 days old and pregnant females were culled for embryo dissection 10 days post-plug. The day of birth was considered P0 and mice were culled for retina extraction 5 days later. Genotyping of *Notch4*^{d1} mice was carried out using primers described in [11]. Primers used to characterise the *Notch4*^{d1} allele were 5'-CGCAGTGTGACTCTGAGGAG-3'

and 5’-TGTCTGTTGTGCCCAGTCAT-3’ (exon 21 to the *Notch4*^{d1} insertion cassette), 5’-CTGGGCACAACAGACAATCGGC-3’ and 5’-TGTCTGTTGTGCCCAGTCAT-3’ (*Notch4*^{d1} insertion cassette), 5’-ATTGCATCGCATTGTCTGAG-3’ and 5’-TCCATCCTCATCCACTTCGGCCTC-3’ (*Notch4*^{d1} insertion cassette to exon 25), 5’-GCTCTTGCCACTCAATTTCCC-3’ and 5’-GCCACCATTCTTGCAGAGTTG-3’ (*Notch4* exon 1-3), 5’-GCTGCACTGTGAGGAGAAGA-3’ and 5’-ATCGAGCAGTGTGTGGACAG-3’ (*Notch4* exon 5-16). *Notch4*$^{-}$ mice were genotyped using primers NeoFwd (5’-TCATTCTCAGTATTGTTTTGCC-3’) and SDRev (5’-CTGGAGAACATGGCCTCATC-3’) and SU (5’-CCTTCCTGGGTCACAGTAGC-3’) and LacZRev (5’-GTCTGTCCTAGCTTCCTCACTG-3’). Reverse transcription was performed using SuperscriptIII (Life Technologies) and oligo-dT according to the manufacturer’s instructions. PCR was performed with Taq polymerase (Roche) according to the manufacturer’s instructions.

2.2. DNA constructs

Notch4 expression plasmids were made by subcloning a XhoI to NotI fragment from pYXNotch4 (I.M.A.G.E clone number 6855960) into pENTR2B (Life Technologies). The 5’ end of Notch4 was amplified using primers 5’-GAGGGGGAATTCCTGAAGAGGGAGAGGAGA-3’ and 5’-ATCGAGCAGTGTGTGGACAG-3’ from C57Bl/6J lung cDNA reverse transcribed using the primer 5’-ATCGAGCAGTGTGTGGACAG-3’ and MonsterScript reverse transcriptase (Epicentre) according to the manufacturer’s instructions. The amplified product was subcloned into the above plasmid using EcoRI and XhoI sites. The 3’ end of Notch4 was amplified from pYXNotch4 using the primers 5’-CACTTGGTCGGTGGACTTG-3’ and 5’-CGCAGCCGGCCGGTTCAGATTTCTTACAACCG-3’ to create an in frame fusion for tagging the C-terminus. pENTR2BNotch4d1 was made by cloning a Notch4 fragment, amplified using the primers 5’-GCTGCACTGTGAGGAGAAGA-3’ and 5’-ATAGCTCGAGATGCAGGTTAGAGGGATTTC-3’, into the XhoI sites of pENTR2BNotch4. pCMXFLAG was generated by cloning annealed oligos 5’-GATCCGACTACAAAGACGATGACGACAAGTAAG-3’ and 5’-CTAGCTTACTTGTCGTCATCGTCTTTGTAGTCG-3’ into the BamHI and NheI sites of pCMX-PL2 [48]. Gateway LR reactions (Life Technologies) were used to transfer the Notch4 and Notch4d1 cDNAs to pCAGiPuroHA and pCMXHA [49] and pCMXFLAG. To generate NOTCH4-Ruby-pCDNA5 FRT/TO AU, Ruby was first PCR amplified from pmRuby-c1 [50] using 5’-TATATGGATCCAACAGCCTGATCAAAGAA-3’ and 5’-TATATGCTAGCTTACCCTCCGCCCAG-3’ and cloned into the BamHI and NheI sites of pCMX-PL2 and subsequently into the inducible vector pCDNA5 FRT/TO AU [51] . pENTR2BNotch4 was

used to gateway clone Notch4 into the resulting vector. pBSN4EP was made by subcloning an EcoRI to PmlI fragment into the EcoRI and SmaI sites of pBluescript II KS(-) (Agilent). Notch1-myc (a gift from Jeff Nye) was cloned into the EcoRI site of pCMX, generating pCMXNotch1myc. A gateway reaction was used to transfer Notch1 from pENTR2BNotch1 into pCMXHA to generate pCMXNotch1HA. pCS2Notch1ΔE-6myc and pCS2Notch4ΔE-6myc were kind gifts from Raphael Kopan [52]. Notch1ΔEHA was made by subcloning a BglII to XhoI fragment of pCMXNotch1HA into BglII to XhoI of pCS2Notch1ΔE-6myc. Notch4ΔEHA was made by subcloning an AflII to NheI fragment of pCMXNotch4HA into the AflII and XbaI sites of pCS2Notch4ΔE-6myc. Notch1ΔE-GVP [53] was modified by removing the Gal4/VP16 sequences by digesting with AscI and religating. A NotI fragment was subcloned from this plasmid into pBluescript II KS(-) (Agilent) to make pBSNotch1:1. A product amplified from pCMXNotch1HA using the primers 5'-CTCGGGCCCACGTAGTCCCACCTG-3' and 5'-AGGGAACCAGAGCTGGCCATGGGC-3' was digested with BamHI and AscI and cloned into the BamHI and AscI sites of pBSNotch1:1. A BamHI to HindIII fragment was then subcloned into pCMXNotch1HA to make the Notch1:1 expression plasmid. A product amplified from pCMXNotch4HA using the primers 5'-CTGCATCTCCACACCCTGT-3' and 5'-AGGGCCCCATGGGCGCGCCGCCGT-3' was digested with XhoI and AscI and subcloned into pBSNotch1:1 to create pBSNotch4:1. A BstEII to NotI fragment was subcloned into pCMXNotch4HA to make the Notch4:1 expression plasmid. A product amplified from pCMXNotch4HA using the primers 5'-ACGGCGGCGCGCCCATGGGGCCCT-3' and 5'-TCCATCCTCATCCACTTCGGCCTC-3' was cut with AflII and AscI and subcloned into the above sites of pBSNotch4:1. A BstEII to AflII fragment was subcloned into pCMXNotch4HA to make the Notch4:4 expression plasmid. The Notch1:4 expression plasmid was made by subcloning an EcoRI to AscI fragment from the Notch1:1 expression plasmid into the Notch4:4 expression plasmid. A 320 bp BamHI fragment from p6×TP1-luc containing six copies of the TP1 sequence [54] was cloned into the BglII site of pGL4.23 (Promega) forming the Notch luciferase reporter pGL4-6×TP1-Luc.

2.3. Cell culture, live imaging and luciferase assays

C2C12 and NIH3T3 lines were grown in DMEM containing 2 mM L-glutamine and 10% FCS in a humidified incubator at 37°C and 5% CO_2. Subconfluent cultures were passaged by detaching the cells with TrypLE Express (Gibco/BRL) and diluting 1/10 every 2-3 days. For transfections cells were seeded at 2.5×10^4 cells per cm^2 and grown overnight at 37°C in a humidified chamber containing 5% CO_2. Cells were transfected with Lipofectamine LTX Reagent following the manufacturer's instructions (Life Technologies). Mouse aortic endothelial cells (MAEC) cells were grown in M199 media containing 2 mM L-glutamine, 10 mM HEPES, 0.1 mg/ml Heparin sodium,

5 ng/ml VEGF and 5% FCS [55] and transfected with Lipofectamine 2000 reagent following the manufacturer's instructions.

For live-cell imaging experiments, C2C12 cells stably expressing a NOTCH1-GFP fusion receptor (NOTCH1-GFP cells) were seeded onto 30 mm round coverslips in 10% FCS in DMEM. The following day cultures were cotransfected with a tetracycline-inducible NOTCH4-Ruby expression construct (NOTCH4-Ruby-pCDNA5 FRT/TO AU) and a Tet Repressor protein expression plasmid (pCDNA6/TR; Life Technologies). Media was replaced on the cells 5 hours post-transfection and left to incubate overnight. A coverslip was transferred to the POCmini imaging apparatus (Pecon). Cells were rinsed in 1 ml Phenol Red-free DMEMgfp media (Evrogen) containing 10% FCS and 1 μg/ml doxycycline and left in a final 1 ml for imaging. Cells were mounted in an incubation chamber at 37°C and 5% CO_2 immediately after addition of doxycycline and left to equilibrate. Images were acquired using a 63× 1.4 NA oil objective on an AxioObserver Z1 Inverted microscope equipped with 710 confocal scan head (Zeiss). Images were captured over the course of 5 hours at 7.5 minute intervals, 1-2 hours after placement in the chamber.

Notch signal transduction was induced by coculturing ligand presenting cells with cultures of responding cells as described elsewhere [49,56,57]. NIH3T3 cells expressing mouse DLL4 were generated by stably transfecting cells with pCAG- mDll4-IRESpuro. Cultures were grown in 1.5 μg/ml puromycin for 10 days, colonies picked and screened by immunofluorescence and immunoblotting for DLL4 expression. Responding cells were seeded at 5×10^4 cells per well into 24-well tissue culture plates and grown overnight. Cells were transfected for 6 hours with pCMXNotch1HA, pCMXNotch4HA or the vector control, plus the Notch responsive reporter pGL4-6×TP1-Luc and the *Renilla* luciferase transfection control, pCMXren [57]. Transfection mixes were aspirated and 5×10^4 ligand presenting cells were added to cultures and incubated overnight. Cocultures were lysed in 100 μl of passive lysis buffer and the luciferase activity was measured using the Dual Luciferase Kit according to the manufacturer's instructions (Promega). Firefly luciferase activity was normalised to the *Renilla* luciferase activity generated from pCMXren.

2.4. C2C12 cell differentiation

C2C12 cells stably expressing NOTCH4HA and NOTCH4d1HA were created by transfecting cells with pCAG-Notch4HA-IRESpuro and pCAG-Notch4d1HA-IRESpuro, respectively. Cultures were grown in 1.5 μg/ml puromycin for 10 days, colonies picked and screened by immunofluorescence and immunoblotting for uniform NOTCH4 expression. Control lines were also generated by stable transfection of pCAG-IRESpuro. Three clones of each Notch4HA, Notch4d1HA and pCAGiPuro were seeded on plastic coverslips (Sarstedt) at 50% confluence per well of a 6-well dish. After 24

hours fresh media was added and cells were grown to confluence over 6 days in 10% FCS DMEM. At days 0, 2, 4 and 6 cells were fixed and stained with MF20 (1/20; DSHB) and TO-PRO 3 (1/1000; Life Technologies).

2.5. Co-immunoprecipitation and western blotting

Co-immunoprecipitations were performed with anti-FLAG antibody (1/150 clone M2; Sigma) or an equal amount of non-specific mouse IgG (Jackson) as described in [58] except that Protein G Dynabeads (Life Technologies) were used. Western blots were carried out with the following antibodies: anti-HA (1/1000, clone 16B12; Covance), anti-myc (1/250, clone 9E10; DSHB), anti-β-Actin (1/5000, clone AC-15; Sigma).

2.6. RACE

The 3'RACE protocol was adapted from [59,60]. One microgram of RNA isolated using the Purelink micro-midi RNA extraction kit (Life Technologies) from neonatal (P5) mouse lung was heat denatured at 65°C for 5 minutes in the presence of 50 pmol of primer 3'RACE primer 5'-CCAGTGAGCAGAGTGACGAGGACTCGAGCTCAAGCTTTTTTTTTTTTTTTTVN-3' and reverse transcribed with SuperScriptIII (Life Technologies) according to the manufacturer's instructions followed by heat inactivation (70°C for 20 minutes) and RNaseH (Life Technologies) treatment for 20 minutes at 37°C. The cDNA was purified with the QIAquick PCR Purification Kit (Qiagen) with an additional 35% guanidine hydrochloride wash. The cDNA was PCR amplified using the primers 5'-CCAGTGAGCAGAGTGACG-3' and 5'-TAGCCAACGCCTTCTACTGC-3' with Platinum Taq (Life Technologies). The PCR conditions were 94°C for 5 minutes followed by 35 cycles of 94°C for 10 seconds, 64°C for 10 seconds and 72°C for 4 minutes and 30 seconds followed by a final incubation at 72°C for 15 minutes. The PCR reaction was purified with the QIAquick PCR Purification Kit (Qiagen) including a wash with 35% guanidine hydrochloride. A nested PCR was performed on 5% of the reaction using the primers 5'-GAGGACTCGAGCTCAAGC-3' and 5'-AGGAGGAGACTGGGATGGAG-3'and Platinum Taq. The PCR conditions were 94°C for 5 minutes followed by 35 cycles of 94°C for 10 seconds, 60°C for 10 seconds and 72°C for 1 minute followed by a final incubation at 72°C for 15 minutes. The resulting PCR product was cloned into pGEMeasyT (Promega) according to the manufacturer's instructions. The cloned product was sequenced using the primers T7 5'-TAATACGACTCACTATAGGG-3' and SP6 5'-ATTTAGGTGACACTATAGAA-3'.

2.7. Northern blotting

Northern blotting was performed as described previously [61]. Neonatal mouse lung RNA was prepared using TRI reagent (Sigma) and separated on a 0.7% denaturing agarose gel before capillary transfer to a Hybond N^+ membrane. An RNA probe was prepared from pBSN4EP by reverse transcription using T7 polymerase (Ambion) and EasyTides Uridine 5'-triphosphate α-^{32}P (PerkinElmer) according to the manufacturer's instructions. Probes were hybridised overnight in 5×SSC, 5×Denhardt's solution, 50% formamide, 1% SDS, 100 μg/ml Torula yeast RNA, 100 μg/ml herring sperm DNA at 60°C. The membrane was washed 3 times in 2×SSC, 0.1% SDS for 15 minutes at room temperature, 2 times in 0.2×SSC, 0.1% SDS at 60°C for 15 minutes and 2 times in 0.2×SSC, 0.1% SDS at 68°C for 15 minutes before exposure to X-ray film. Bands were quantified using ImageJ software.

2.8. RNA *in situ* hybridisation, LacZ staining and wholemount immunofluorescence

RNA *in situ* hybridisation was performed as described previously [62]. The probe against exons 1-5 of *Notch4* was made using an EcoRI linearised pBSN4EP template DNA and T7 RNA Polymerase. LacZ staining was performed on fixed embryos (10 minutes in 0.2% glutaraldehyde, 0.1 M phosphate buffer (pH 7.3), 2 mM $MgCl_2$, 5 mM EGTA) washed twice for 10 minutes in 0.1 M Na phosphate buffer (pH 7.3), 2 mM $MgCl_2$, 0.1% Na deoxycholate, 0.02% NP40 and stained in wash buffer containing 0.232 mM NaCl, 5 mM $K_3Fe(CN)_6$, 5 mM $K_4Fe(CN)_6$, 0.24 mg/ml spermidine, 1 mg/ml X-gal for 72 hours at 37°C. Stained embryos were washed and photographed. Wholemount immunofluorescence on neonatal mouse retinas was performed as follows. Mouse pups at 5 days post birth were sacrificed by decapitation and tail clips taken for genotyping. Eyes were enucleated and fixed in 4% PFA at 4°C for 10 minutes on ice. An incision was made using dissecting forceps just below the lens and the pigmented epithelium and outer layers removed. The vitreous and associated hyaloid vasculature were removed and the dissected retina was fixed for a further 2 hours in 4% PFA at 4°C followed by three 5 minute washes in PBS. Non-specific binding was prevented by incubation for 1 hour at room temperature in Block (5% donkey serum, 0.3% Triton X-100 in PBS). Anti-PECAM1 (1/200, clone MEC13.3; BD Biosciences) and anti-ACTA2 (1/100, clone 1A4, Dako) were diluted in Block, added to retinas and incubated with gentle agitation overnight at 4°C. The retinas were washed six times for 15 minutes in PBST (PBS containing 0.1% Triton X-100) then incubated with anti-mouse 488 and anti-Rat Cy3 secondary antibodies (1/500; Jackson) for 2 hours at room temperature in the dark. Following six 15 minute washes in PBST at room temperature, four radial cuts were made in the retina to allow it to be laid flat on a microscope slide. The retinas were then mounted in ProLong Gold Antifade reagent (Life Technologies). Retinas were either imaged as z-stacks in a 3×3 tile using a 10× 0.45 NA objective or in a 6×6 tile using a 20× 0.8 NA objective on an AxioObserver Z1 microscope fitted with a 710 confocal scan head

(Zeiss). NOTCH4 reactivity was detected in retinas using anti-NOTCH4 (1/2000, clone HMN4-14; iCyt) and tertiary amplification with biotinylated donkey anti-armenian hamster secondary antibody (1/1000; Jackson) followed by Cy3-conjugated streptavidin (1/1000; GeneTex) in conjunction with endothelial staining using Alexa-488 *Griffonia simplicifolia* Isolectin B4 (1/200; Life Technologies).

2.9. Image analysis and statistics

Z-stacks were maximum intensity projected using the Zen 2009 software (Zeiss) and then thresholded and converted to a binary format in ImageJ (NIH). The perimeter of the vascular bed was defined as a region-of-interest in ImageJ using the tracing tool. The vascular area was determined by dividing the area within this perimeter by the mean area of the heterozygotes within each litter. Litters were excluded if they contained fewer than two heterozygotes. Rapid Analysis of Vessel Elements (RAVE) software was used to quantify changes in the organisation of the vasculature [63]. Maximum intensity projected images were subjected to a 2 pixel Gaussian Blur in ImageJ then converted to binary format. All non-contiguous pixels positive for PECAM1 were excluded from analysis. Size values were set to 1 in RAVE. Sigma and maximum radius inputs were set at 5 and 30, respectively. Total vessel length and fractal dimension was determined by RAVE. Vessel length density was expressed as the ratio of total vessel length to vascular area for individual retinas. In order to correct for inter-litter variation, all measurements are shown relative to the mean of the heterozygotes in each mouse litter. Litters were excluded from further analysis if they contained fewer than two heterozygotes.

Measurements were analysed using two-tailed unpaired Student's T-test with PRISM software (Graphpad) and considered significantly different if $P < 0.05$.

3. Results

3.1. *Notch4*^{d1} mice express a truncated *Notch4* transcript

In the course of studying the role of *Notch4* during mouse embryogenesis, we examined its expression pattern by RNA *in situ* hybridisation using a probe designed against the 5' end (exons 1-5) of the *Notch4* transcript (Fig. 1A; ex1/5 probe). To demonstrate that the probe was specific to *Notch4*, embryos homozygous for the published *Notch4* allele (*Notch4*^{tm1Grid}; hereafter termed *Notch4*^{d1}) were included in our analysis as a negative control [11]. *Notch4*^{d1} is the only reported knockout allele of *Notch4* and lacks exons 22 and 23; it was designed to prevent transcription of downstream sequences encoding the NOTCH4 intracellular domain (NOTCH4 ICD) [11]. We observed that *Notch4* transcripts were largely restricted to the vasculature as reported, and at E10.5

were most obvious in the intersomitic vessels (Fig. 1B; [37,46]). In addition to its vascular expression, we observed *Notch4* expression in a caudal site not previously reported. In this region *Notch4* was expressed in the tail bud and in the presomitic mesoderm (Fig. 1B). Unexpectedly, *Notch4* transcripts were also detected in *Notch4*$^{d1/d1}$ embryos suggesting that the *Notch4*^{d1} allele produced a stable transcript in the same pattern as *Notch4*$^{+/+}$ embryos (Fig. 1B). Genomic PCR with primers amplifying within the targeted region (Fig. 1C; ex22), within the selection cassette (Fig. 1C; neo) as well as flanking the 5' and 3' recombination sites (Fig. 1C; ex21/neo and neo/ex25) confirmed that the *Notch4*^{d1} allele was targeted as reported [11]. To confirm that the *Notch4*^{d1} locus produces a transcript, reverse transcription PCR (RT-PCR) was performed on oligo-dT primed neonatal lung cDNA of each genotype produced by *Notch4*$^{+/d1}$ intercross. Primers amplifying within the targeted region (Fig. 1D; ex22) confirmed that exon 22 was not transcribed in *Notch4*$^{d1/d1}$ mice. Primers amplifying exons 1 to 3 (Fig. 1D; ex1/3) and exon 15 to 16 (Fig. 1D; ex15/16) upstream of the targeting cassette produced PCR products in all three genotypes, indicating that the *Notch4*^{d1} allele produced a spliced and polyadenylated transcript that included at least exons 1 to 16 of the *Notch4* gene. To determine the extent of this transcript we performed 3' Rapid Amplification of cDNA Ends (RACE) PCR on *Notch4*$^{d1/d1}$ neonatal lung cDNA. A single RACE product was amplified and found to be a fusion mRNA between *Notch4* and the neomycin (neo) selection cassette (Fig. S1A). An identical transcript was found in all mice tested (n=6). The transcript was polyadenylated 18 nucleotides 3' of the SV40 polyadenylation signal of the *neo* cassette. Exon 21 of the *Notch4* locus was spliced to a cryptic 3' intron acceptor within the *neo* cassette. The *Notch4* open reading frame continued into the *neo* gene encoding an additional 10 amino acids before encountering a termination codon. An additional cryptic exon is present in the 3'UTR of the transcript 51 nucleotides downstream of the termination codon. Nonsense mediated decay causes the degradation of mRNAs harbouring termination codons more than 50-55 nucleotides from an exon-exon junction [64]. It was therefore possible that we had simply detected a residual transcript left over following nonsense mediated decay although we did not observe reduced expression in *Notch4*^{d1} embryos by RNA *in situ* hybridisation (Fig. 1B). To exclude this possibility and to confirm that the single transcript we isolated by RACE (Fig. S1A) was unique, we performed northern blot analysis using a probe upstream of the targeting site encompassing exons 1 to 5. A single *Notch4* transcript was detected in *Notch4*$^{+/+}$ lung (Fig. 1E). A single faster migrating transcript was detected in *Notch4*$^{d1/d1}$ lung and in *Notch4*$^{+/d1}$ both transcripts were detected. *Notch4* transcripts were overexpressed 2.6-fold in *Notch4*$^{d1/d1}$ and 1.7-fold in *Notch4*$^{+/d1}$ lung (Fig. 1F). In summary, these data demonstrate that the *Notch4*^{d1} allele overexpresses a truncated *Notch4* transcript.

3.2. *Notch4*^{d1} mice overexpress a truncated NOTCH4 protein

The truncated transcript expressed by the *Notch4*^{d1} allele is predicted to encode most of the extracellular domain of the receptor including all 29 EGF-like repeats and the Lin12-Notch repeats LNR-A and LNR-B followed by 10 amino acids (Fig. S1A). This putative NOTCH4d1 protein therefore lacks the third LNR repeat (LNR-C), heterodimerisation domain (HD), transmembrane domain and the intracellular domain (Fig. S1B). To determine if the *Notch4*^{d1} allele produced a stable protein, we performed wholemount immunofluorescence to detect NOTCH4 protein in the retinal vasculature; a known domain of *Notch4* mRNA expression [65]. Retinas from 5 day old (P5) *Notch4*$^{+/+}$, *Notch4*$^{+/d1}$ and *Notch4*$^{d1/d1}$ mice were stained with an antibody that specifically detects the extracellular domain (EC) of mouse NOTCH4 (Fig. S2) and fluorescently labelled *Griffonia simplicifolia* Isolectin B4 to mark the vasculature. In wildtype retinas, NOTCH4 reactivity was detected in the developing arteries and veins (Fig. 2A,B,D), similar to expression of the transcript [65]. However, NOTCH4 reactivity was also found in capillaries. NOTCH4 expression was strongest in the newly laid down primary plexus at the periphery of the developing vasculature, compared with more mature vessels closer to the optic nerve that had undergone remodelling (Fig. 2C, Fig. S2B). Tip and stalk cells in the primary plexus both expressed NOTCH4, as did filopodial extensions from the tip cells (Fig. 2E). NOTCH4 reactivity was detected in the developing arteries of *Notch4*$^{d1/d1}$ retinas, demonstrating that a NOTCH4 protein is produced by the *Notch4*^{d1} allele (Fig. 2D). Interestingly, *Notch4*$^{+/+}$ retinas exhibited much weaker reactivity and *Notch4*$^{+/d1}$ mice showed intermediate expression. Thus, the *Notch4*^{d1} allele overexpressed a truncated form of NOTCH4.

3.3. NOTCH4 and NOTCH4d1 inhibit signalling via NOTCH1

The *Notch4*^{d1} allele expresses a truncated NOTCH4 protein lacking the intracellular domain and therefore cannot transduce a canonical Notch signal. It also lacks the transmembrane domain and is therefore soluble and possibly secreted. Addition of soluble Notch extracellular domain protein inhibits ligand-dependent Notch signalling [66-68], implying that soluble forms of NOTCH4 such as NOTCH4d1 could inhibit Notch signalling. In addition, the NOTCH1 extracellular domain inhibits ligand-induced signal transduction when expressed in cells coexpressing (that is, *in cis*) the complete NOTCH1 receptor [66]. Given that the NOTCH4d1 protein includes most of the extracellular domain, we were interested to determine if it could similarly inhibit Notch signalling when expressed *in cis*. We performed Notch signal transduction assays in which cells expressing DLL4 were cocultured with NIH3T3 cells expressing various combinations of *Notch4*, *Notch4*^{d1} *or Notch1* cDNAs and a synthetic Notch responsive luciferase reporter. As expected, NOTCH1 robustly activated the luciferase reporter when cocultured with DLL4 cells (Fig. 3A; lane 8). Unsurprisingly, NOTCH4d1, which lacks the ICD required for signalling, did not activate the

Notch reporter above control (Fig. 3A; lane 7). However, NOTCH4 also failed to elicit a signal upon coculture with DLL4 cells (Fig. 3A; lane 6). We confirmed that NOTCH4 could not signal in endothelial cells (Fig. S3A) or in non-endothelial cells in response to JAG1 expressing cells (Fig. S3B). Even artificial activation of signalling by EDTA [69] failed to elicit a detectable signal from NOTCH4 (Fig. S3C).

We were unable to induce NOTCH4 signalling in cultured cells. This inability to signal may reside in the intracellular domain or extracellular domain. NotchΔE constructs span the membrane but lack the LNR, HD and EGF-like repeats. Such truncated receptors are constitutively active in the absence of ligand and thus constitute a means to test the ability of a Notch receptor to be S3-cleaved and subsequently activate Notch target gene transcription [27]. We compared the signalling capacity of NOTCH4ΔE to NOTCH1ΔE by transfecting these constructs into NIH3T3 cells. NOTCH4ΔE induced the Notch reporter 480-fold over the vector control compared with over 5000-fold activation by NOTCH1ΔE (Fig. 3B), consistent with previous reports using ICD constructs [32,35,36]. Thus, once released, NOTCH4ICD does transduce a signal albeit at a lower level than NOTCH1ΔE, suggesting that NOTCH4ICD is not released at detectable levels from NOTCH4 in response to ligand. To investigate this further, chimaeric receptor constructs, in which the intracellular domains C-terminal to the S3-cleavage site were swapped (referred to as NOTCH1:4 and NOTCH4:1; Fig. 3C), were tested in Notch signalling assays. Ligand cells activated NOTCH1:4 by 5-fold, significantly lower than NOTCH1:1 (Fig. 3C). Nevertheless when placed in the context of a functional receptor NOTCH4ICD can transduce a signal. By contrast, NOTCH4:1 only activated the Notch reporter 2-fold in response to ligand, despite the presence of the strong transactivation domain of NOTCH1ICD (Fig. 3C). These data indicate that in response to ligand, the NOTCH4 extracellular domain fails to release detectable levels of NOTCH4ICD.

Not only did NOTCH4 lack signalling capacity but also expression of *Notch4* with *Notch1* inhibited NOTCH1-dependent signal transduction (Fig. 3A; lane 9) and did so in a dose-dependent manner (Fig. S3D). This inhibition was not due to competition for promoter binding between the NOTCH1ICD and NOTCH4ICD because transfection of increasing amounts of NOTCH4ΔE did not reduce ligand-induced NOTCH1 signalling and instead increased signal output in a synergistic manner (Fig. 3D). Consistent with this, NOTCH4d1, which lacks the intracellular domain also inhibited activation of NOTCH1 by DLL4 expressing cells (Fig. 3A; lane 10). Thus, NOTCH4 could not transduce a signal itself but inhibited signalling via NOTCH1 and this effect was not mediated by the NOTCH4ICD. Importantly, the truncated form of NOTCH4 overexpressed by the *Notch4*^{d1} allele retains this novel inhibitory function.

Our Notch signal transduction assays demonstrated that NOTCH4 and NOTCH4d1 inhibited NOTCH1 signalling. To determine if this inhibition induces a biological response, we

examined C2C12 myoblast differentiation into myocytes and myotubes as this is prevented by Notch signalling [70]. We generated C2C12 cell lines that stably express NOTCH4 or NOTCH4d1. These cell lines were difficult to maintain in an undifferentiated state and precociously differentiated under suboptimal differentiation conditions compared to control cell lines (Fig. 3E). This finding is consistent with NOTCH4 and NOTCH4d1 inhibiting Notch signal transduction and demonstrates that this inhibitory activity can alter biological processes such as myoblast differentiation.

NOTCH4 might inhibit NOTCH1 through interaction. Interaction between NOTCH4 and NOTCH1 could inhibit NOTCH1 signalling by interfering with the processing of NOTCH1. Full-length NOTCH1 is processed in the TGN by FURIN or a FURIN-like convertase to form a heterodimer [23,24]. Only heterodimeric NOTCH1 is presented on the cell surface and is competent to receive signal [23-25,71]. Therefore, to determine if NOTCH4 interacts with NOTCH1, we transfected C2C12 cells stably expressing HA-tagged NOTCH1 with FLAG-tagged NOTCH4 and immunoprecipitated with anti-FLAG antibody. Full-length NOTCH1 specifically coprecipitated with NOTCH4 (Fig. 4A, lane 7). However, processed, heterodimeric NOTCH1 did not coprecipitate with NOTCH4 even though it was present in lysates (Fig. 4A, lanes 2 and 3). NOTCH4d1 also interacted with full-length NOTCH1 (Fig. 4A, lane 9). Taken together these data indicate that NOTCH4 interacts exclusively with the unprocessed full-length form of NOTCH1. Since NOTCH4d1 also interacted with full-length NOTCH1, this interaction must not rely on regions of NOTCH4 that are absent in NOTCH4d1; that is, regions C-terminal to LNR-B (Fig. S1B).

NOTCH4 interacts with the unprocessed, full-length form of NOTCH1 suggesting that these proteins interact before reaching the TGN because NOTCH1 is S1-processed in the TGN[23]. We performed live-cell imaging experiments to observe the localisation of NOTCH1 in the absence and presence of NOTCH4. A fusion between NOTCH4 and the red fluorescent protein mRuby was created and cloned into a tetracycline inducible expression vector. NOTCH4-Ruby was transfected into C2C12 cells that stably express a NOTCH1-GFP fusion receptor and fluorescence was imaged following induction with the tetracycline analogue doxycycline. NOTCH1-GFP was localised to the plasma membrane and in cytoplasmic vesicles that were concentrated close to the nucleus in uninduced cells, a pattern that is indistinguishable from untagged NOTCH1 (Fig. 4B, 0 min) [58]. Once induced, NOTCH4-Ruby was localised in a cytoplasmic network characteristic of the endoplasmic reticulum (ER) but also in large cytoplasmic structures (Fig. 4B, 150 and 300 min). Upon induction of NOTCH4-Ruby, the subcellular localisation of NOTCH1-GFP changed to match that of NOTCH4-Ruby (Fig. 4B; movie 1). Taken together these data suggest that NOTCH4 binds unprocessed, full-length NOTCH1 and in doing so alters the subcellular localisation of NOTCH1.

This suggests that NOTCH1 would not be efficiently S1-processed in cells expressing NOTCH4. To investigate this, we transfected increasing amounts of *Notch4* into a NIH3T3 cell line stably expressing myc-tagged NOTCH1 and examined S1-processing of NOTCH1 by western blot (Fig. 4C). As the amount of transfected *Notch4* increased, we observed increasing levels of unprocessed full-length NOTCH1 (Fig. 4D). The ratio of full-length to heterodimeric NOTCH1 also increased with increasing amounts of *Notch4* transfected (Fig. 4D). The levels of heterodimeric NOTCH1 stayed constant, most likely due to the protein's inherent stability [24]. These data indicate that NOTCH4 interacts with full-length NOTCH1, alters its trafficking and perturbs its S1-processing. [insert movie 1 here]

3.4. Generation of mice with a definitive *Notch4* null allele

Mice homozygous for the $Notch4^{d1}$ allele ($Notch4^{d1/d1}$) are viable and fertile [11]. We have found that a truncated NOTCH4 protein is expressed from the $Notch4^{d1}$ allele, at levels greater than those produced by the *Notch4* allele. Importantly, like NOTCH4, NOTCH4d1 inhibits Notch signalling (Fig. 3A). Therefore, the role of *Notch4 in vivo* warrants further study.

To determine the phenotype of mice lacking *Notch4* we generated mice from embryonic stem (ES) cells targeted to replace the entire *Notch4* coding sequence with *LacZ* and *neo* expression cassettes (Fig. 5A). This null allele $Notch4^{tm1(KOMP)Vlcg}$ will be referred to as $Notch4^{-}$. Mice homozygous for this *Notch4* null allele ($Notch4^{-/-}$) were born at expected Mendelian ratios and were viable and fertile (not shown). We confirmed that the *Notch4* locus was targeted correctly by performing genomic PCR with primers amplifying exon 22 of *Notch4* (Fig. 5B; ex22), and flanking the 5' and 3' recombination sites (Fig. 5B; 5'/LacZ and neo/3'). These PCR products were sequenced to confirm the insertion site of the targeting cassette (data not shown). NOTCH4 is not produced from the null allele as reactivity to anti-NOTCH4 EC antibody could not be detected in $Notch4^{-/-}$ tissue (Fig. S2B). Like the *Notch4* transcript (Fig. 1B), β-galactosidase activity driven from the *Notch4* promoter was detected in the vasculature of the head and in intersomitic vessels as well as the tail bud and presomitic mesoderm of $Notch4^{-/-}$ E10.5 embryos but not $Notch4^{+/+}$ embryos (Fig. 5C-F).

Although $Notch4^{-/-}$ mice were viable, it is possible that the vasculature might differ from that of $Notch4^{+/+}$ mice. We therefore examined postnatal retinal angiogenesis in the mouse as it proceeds in a defined spatio-temporal manner and is quantifiable [72,73]. The vasculature at P5, as highlighted by anti-PECAM1 reactivity, had grown about three quarters of the way to the edge of the retina and was undergoing remodelling as the initial plexus forms a mature vascular bed. At this stage smooth muscle cell investment, as detected by ACTA2 expression (Fig. 6A, B), was restricted to the arteries. We compared the effects of the two *Notch4* alleles *($Notch4^{-}$, $Notch4^{d1}$)* on angiogenesis by staining retinas from P5 mice with antibodies to PECAM1 and ACTA2. ACTA2

staining was not overtly different between genotypes (Fig. 6A, B). The extent of vascular growth was assessed by measuring both total vessel length within each retina as well as the area covered by the vascular plexus. *Notch4*$^{+/d1}$ and *Notch4*$^{d1/d1}$ retinas showed a reduction in the area covered by vasculature (18.0%; P=0.003 and 17.4%; P=0.022, respectively) and a reduction in total vessel length (16.9%; P=0.006 and 18.7%; P=0.018, respectively) compared with *Notch4*$^{+/+}$ littermates (Fig. 6A, C, D). *Notch4*$^{+/-}$ and *Notch4*$^{-/-}$ retinas exhibited a reduction in vascular area (10.9%; P=0.011 and 13.0%; P=0.030, respectively) compared with *Notch4*$^{+/+}$ littermates (Fig. 6B, F). *Notch4*$^{+/-}$ and *Notch4*$^{-/-}$ retinas also exhibited reduced vessel length (9.7% and 9.8%) compared to *Notch4*$^{+/+}$ littermates (Fig. 6B, G). However, this difference only reached statistical significance in the *Notch4*$^{+/-}$ and not the *Notch4*$^{-/-}$ retinas (P=0.0153 *vs*. 0.0636). These data indicate that growth of the vasculature is delayed in mice carrying either *Notch4* allele, although mice carrying the *Notch4*^{d1} allele are more delayed than *Notch4*$^{-/-}$ mice. Vessel length density, the ratio of vessel length to vascular area independent of vessel thickness (Fig. 6E, H), and fractal dimension, a measure of the tortuosity of the vasculature (not shown), were similar between all *Notch4*$^{+}$, *Notch4*^{d1} and *Notch4*$^{-}$ genotypes.

4. Discussion

NOTCH4 is almost exclusively expressed in vascular endothelial cells, unlike NOTCH1, which is expressed in most tissues. Despite this, NOTCH4 is the least studied of the mammalian Notch receptors and accordingly the least understood in terms of its signalling potential and function. In cultured cells NOTCH4 has been reported to signal in response to ligand by some but not all laboratories [38,39,74]. The *Notch4* knockout allele indicates in mice that *Notch4* has a minor role in embryonic angiogenesis (only on a *Notch1* null background) and contributes to initial tumour perfusion [11,44]. Therefore, we further investigated NOTCH4 signal transduction and its role during angiogenesis, and made some surprising findings.

Firstly, we discovered that the reported *Notch4* knockout allele *(Notch4*^{d1}*)* produced a transcript encoding virtually all the NOTCH4 extracellular domain. This transcript has the same vascular expression pattern as the wildtype *Notch4* allele in the mouse embryo and is expressed at a 2-fold greater level than wildtype. For the first time we also document the expression pattern of the NOTCH4 protein in the developing retinal vasculature (Fig. 2). NOTCH4 was predominantly found at the growing vascular front with lower expression in established capillary beds. At the growing vascular front, NOTCH4 was present in both stalk and tip cells. Although overexpressed, the distribution of the NOTCH4d1 protein was similar to NOTCH4 (Fig. 2).

We next demonstrated that NOTCH4 was unable to be activated by ligand using a coculture assay where cell-bound ligand is presented to Notch-expressing cells and canonical signal

transduction is measured by a CSL-binding transcriptional reporter assay (Fig. 3). NOTCH4 was not activated in a variety of cell lines including an arterial endothelial line (Fig. S3). Moreover, we were even unable to detect NOTCH4 signal transduction after incubation with EDTA (Fig. S3), which is a powerful activator of NOTCH1 due to its ability to chelate calcium ions and thus unfold the negative regulatory region [69,75]. That we could not induce NOTCH4 signal transduction is consistent with the findings of Aste-Amezaga et al. (2010) who could not detect ligand-induced signalling from a Notch4-GAL4 activation domain fusion construct although similar constructs based on Notch1-3 could signal [74]. Additionally, while expression of the activated form of NOTCH4 (NOTCH4ICD) could induce microvessels and expression of *Jag1* and *Notch4* itself, full-length NOTCH4 had no effect [76]. However, in contrast to our findings and that of others, NOTCH4 is reported to activate CSL-dependent reporter transcription by 3.8-fold upon addition of DLL4 expressing cells [38] and upregulate Notch target genes *Flt4*, *Hey1* and *Hey2* in response to both DLL4 and JAG1 [39]. It is not apparent why these reports are in contrast but they likely reflect differences in cell type, means and extent of NOTCH4 overexpression, culture conditions and methods of detecting signal transduction.

We obtained a good understanding of how the extracellular and intracellular domains of NOTCH4 function by examining the activity of constitutively active NOTCH4 and NOTCH1 and by generating chimaeric Notch receptors. Firstly, we showed that a constitutively active version of NOTCH4 (NOTCH4ΔE) is a poor activator of transcription compared with NOTCH1ΔE (Fig. 3). This could be because NOTCH4ΔE may not be efficiently γ-secretase cleaved compared to NOTCH1ΔE. However, the intracellular domains of the Notch paralogues also display a range of activation strengths on a variety of promoters *in vitro* [32,35,36] and *in vivo* [77]. Both NOTCH1 and NOTCH2 contain sequences in the C-terminal region that act as a transcriptional activation domain (TAD). In the case of the NOTCH3, its intracellular domain requires a nearby zinc finger binding site before it displays transactivation activity [36]. No such requirement has been reported for NOTCH4 and no TAD has been identified. NOTCH4, like NOTCH3, may also require additional factors to efficiently activate transcription.

Next, we showed that a NOTCH4:1 chimaeric receptor does not signal as strongly as a NOTCH1:4 chimaera. Chimaeric NOTCH4:1 contains all of the protease cleavage sites of NOTCH4 and therefore measures the ability of NOTCH4 to respond to ligand, detected by the strong transactivation activity of NOTCH1ICD. This chimaeric receptor generated low-level reporter activity indicating that, in the context of the complete NOTCH4 receptor, ligand can induce minimal receptor activation and ICD generation. In the NOTCH1:4 chimaera we exploited NOTCH1's ability to signal in response to ligand to measure the ligand induced signalling potential of NOTCH4ICD. In this chimaera addition of NOTCH4ICD to NOTCH1 produced a somewhat

improved transcriptional response compared with NOTCH4:1 or NOTCH4:4. Observations from both chimaeras indicate that differences between the extracellular domains of NOTCH4 and NOTCH1 are the primary cause of the lack of NOTCH4 signal transduction. The fact that constitutively active NOTCH4ΔE undergoes S3-cleavage [52] implies that the NOTCH4 extracellular domain is defective upstream of this event.

Further analysis of Notch signalling revealed that NOTCH4 inhibited ligand-induced NOTCH1 signal transduction in cultured cells (Fig. 3). Moreover, NOTCH4 inhibited the Notch-mediated inhibition of C2C12 myoblast differentiation (Fig. 3). This is the first demonstration of a complete Notch receptor inhibiting the signal transduction of another Notch receptor, when expressed in the same cell. Notch signalling is also inhibited when DSL ligands are expressed in the same cell as the receptor, a phenomenon termed *cis*-inhibition. This *cis*-inhibition by DSL ligands regulates Notch signal output separate from their ability to induce signalling *in trans*, and is important for Notch-dependent lateral inhibition and boundary formation in *Drosophila*, and perhaps vertebrates as well [58,78]. Our findings indicate that *cis*-inhibition, not only via DSL ligands but via other Notch receptors, also regulates Notch signal transduction. The significance of such receptor-mediated *cis*-inhibition *in vivo* is currently not known. However, retention of NOTCH4 *cis*-inhibitory activity in *Notch4*$^{d1/d1}$ mice may explain the reduced extent of vasculature of *Notch4*$^{d1/d1}$ retinas at P5 compared with those of *Notch4*$^{-/-}$ mice. Further comparison of *Notch4*$^{d1/d1}$ and *Notch4*$^{-/-}$ mice should provide insight into the contribution of receptor *cis*-inhibition to the overall function of NOTCH4 *in vivo*.

We established that the intracellular domain of NOTCH4 (NOTCH4ICD) did not inhibit NOTCH1 signalling (Fig. 3). This indicates that the NOTCH4 extracellular domain mediated the inhibition. This is consistent with our finding that NOTCH4d1 inhibited NOTCH1 signalling in ligand-induced signalling assays as well as in the myoblast differentiation assay (Fig. 3), as NOTCH4d1 consists only of the extracellular part of NOTCH4. Whilst investigating the mechanism of inhibition, we demonstrated that NOTCH4 (as well as NOTCH4d1) interacts with full-length (unprocessed) NOTCH1 and that this interaction leads to an accumulation of unprocessed NOTCH1 (Fig. 4); this form of NOTCH1 cannot signal [25,71] and thus this interaction might explain how NOTCH4 inhibits NOTCH1 signalling. There are reports of Notch receptors forming dimers. For example, NOTCH1 and NOTCH2 can be co-immunoprecipitated with NOTCH1 [79-81]. As in our study, the captured receptor is full-length and thus not S1 processed, and virtually all of it is intracellular. Since FURIN cleavage of NOTCH1 occurs in the TGN [23] and full-length NOTCH1 is largely localised to the ER [81], dimerisation likely occurs early in the trafficking pathway, prior to reaching the TGN.

We postulated that the intracellular interaction of NOTCH4 and NOTCH1 might cause the inhibition of NOTCH1 signalling by interfering with the processing of NOTCH1 and its subsequent trafficking. If this were the case then NOTCH4 would be likely to disrupt the subcellular localisation of NOTCH1. NOTCH1 is localised in intracellular vesicles and to a lesser degree on the cell surface [58] and is constantly internalised and recycled [82,83]. Using live-cell imaging we show that NOTCH1 was mostly localised in intracellular puncta and that induction of NOTCH4 in NOTCH1-expressing cells changed the localisation of NOTCH1 to the same subcellular regions as NOTCH4 in cells expressing both proteins (Fig. 4). The loss of NOTCH1 positive vesicles available to participate in signalling could therefore explain the inhibition of NOTCH1 signalling by NOTCH4.

The above findings lead us to propose a model of how NOTCH4 contributes to canonical Notch signal transduction. In terms of signal transduction, NOTCH4 lacks detectable transactivating activity compared with NOTCH1 because its extracellular domain fails to sufficiently generate the ICD fragment. With respect to inhibition of signal transduction, NOTCH4 binds and sequesters full-length NOTCH1 preventing it from being S1-processed. It is interesting to note that *Notch4* expression is under the transcriptional control of canonical Notch signalling. The *Notch4* promoter contains CSL binding sites [84] and *Notch4* expression is upregulated by transfection with NotchICD constructs [40,76]. Thus NOTCH4 may serve to attenuate NOTCH1 signalling in a negative feedback loop in a similar manner to the Notch target Nrarp [33,85].

Approximately 50% of *Notch4*$^{d1/d1}$;*Notch1*$^{-/-}$ mutants have a more severe phenotype than *Notch1*$^{-/-}$ alone, suggesting NOTCH4 can function redundantly with NOTCH1 during embryogenesis [11]. Affected embryos were found to have fewer somites, open neural tubes and had not completed turning. In the vasculature the anterior cardinal vein had collapsed [11]. This is seemingly at odds with our finding that the primary function of NOTCH4 is as an inhibitor of NOTCH1. However, it is also possible that NOTCH4 may signal as a secondary role. We find that while NOTCH4 could not signal in cell culture, minimal signalling can be induced via the NOTCH4 EC if fused with NOTCH1 ICD. Therefore, there may be circumstances *in vivo* that allow NOTCH4 to produce an effective signal and thus support NOTCH1's role during angiogenesis.

Finally we showed that NOTCH4 does not play a major role in embryonic angiogenesis as we generated mice null for *Notch4* and they survived. We have however revealed a mild angiogenic phenotype in the retinas of *Notch4* null mice and those homozygous for the *Notch4*^{d1} allele. The extent of vessel coverage in *Notch4*$^{-}$ and *Notch4*^{d1} retinas at P5 is reduced, suggesting that there is a delay in the growth of the vascular plexus at this stage. This finding is consistent with the expression of the NOTCH4 receptor that we report at the newly forming vascular front. Inhibition of Notch signalling, via administration of γ-secretase inhibitors, anti-Dll4 neutralising antibody, or

reduced *Dll4* dosage increases the number of tip cells and results in a more dense network [17-19]. Thus removal of *Notch4*, which we report is an inhibitor of NOTCH1, may be expected to reduce vascular density. Our finding that the density of the vasculature is not significantly altered by loss of *Notch4* is at odds with this. Although a direct quantitative comparison of Notch receptor expression *in vivo* is not possible, we find it much harder to detect transcript and protein of Notch4 than Notch1 in the embryo or postnatal retina. This indicates that expression of *Notch4* is much lower than that of *Notch1* during development. This might explain why the mild angiogenic phenotype in the *Notch4*$^{-/-}$ retina is not consistent with the loss of a NOTCH1 inhibitor. Thus loss of *Notch4* may have more dramatic phenotypic consequences under conditions that cause induction of NOTCH4 expression or in tissues that normally express high levels of NOTCH4.

Although we have not revealed a major role for *Notch4* in developmental angiogenesis, our findings are important as all knowledge to date about this receptor *in vivo* is based on mouse lines that either overexpress the constitutively active form of the receptor (which is not physiological) or that carry an allele that is considered to be null, but that rather overexpresses the extracellular domain of the receptor [9,11,40,41,44,86]. Whether NOTCH4 functions in various scenarios where angiogenesis occurs in the adult remains to be tested; this can now be confidently examined using the *Notch4* null mice that we have generated.

Acknowledgements

We wish to thank Urban Lendahl for cell lines and reagents, Tom Gridley and The Jackson Laboratory for *Notch4*^{d1} mice, Hiroko Inoue for the MAEC cell line, Jörg Wiedenmann for the pmRuby-c1 plasmid, Stuart Pitson for the pCDNA5 FRT/TO AU plasmid, the BioCORE staff for animal care, and Herbert Smith for generously donating the confocal microscope used in this study. The work was supported by the Australian National Health and Medical Research Council: Project Grant 1003209; Postgraduate Scholarship with the National Heart Foundation 573738, Senior Research Fellowships 514900 and 1042002 and The Cancer Institute of NSW fellowship 06/ECF/1-03. The ES cells used for this research project were generated by the trans-NIH Knock-Out Mouse Project (KOMP) and obtained from the KOMP Repository (www.komp.org). NIH grants to Velocigene at Regeneron Inc (U01HG004085) and the CSD Consortium (U01HG004080) funded the generation of gene-targeted ES cells for 8500 genes in the KOMP Program and archived and distributed by the KOMP Repository at UC Davis and CHORI (U42RR024244).

References

[1] J. Folkman, Angiogenesis: an organizing principle for drug discovery? Nat. Rev. Drug Discov. 6 (2007) 273–286.

[2] P. Carmeliet, Angiogenesis in life, disease and medicine, Nature. 438 (2005) 932–936.

[3] I. Sörensen, R.H. Adams, A. Gossler, DLL1-mediated Notch activation regulates endothelial identity in mouse fetal arteries, Blood. 113 (2009) 5680–5688.
[4] M. Ehling, S. Adams, R. Benedito, R.H. Adams, Notch controls retinal blood vessel maturation and quiescence, Development. 140 (2013) 3051–3061.
[5] Y.H. Kim, H. Hu, S. Guevara-Gallardo, M.T.Y. Lam, S.-Y. Fong, R.A. Wang, Artery and vein size is balanced by Notch and ephrin B2/EphB4 during angiogenesis, Development. 135 (2008) 3755–3764.
[6] L. Chang, M. Noseda, M. Higginson, M. Ly, A. Patenaude, M. Fuller, et al., Differentiation of vascular smooth muscle cells from local precursors during embryonic and adult arteriogenesis requires Notch signaling, Proc. Natl. Acad. Sci. USA. 109 (2012) 6993–6998.
[7] B. Cristofaro, Y. Shi, M. Faria, S. Suchting, A.S. Leroyer, A. Trindade, et al., Dll4-Notch signaling determines the formation of native arterial collateral networks and arterial function in mouse ischemia models, Development. 140 (2013) 1720–1729.
[8] A. Limbourg, M. Ploom, D. Elligsen, I. Sörensen, T. Ziegelhoeffer, A. Gossler, et al., Notch ligand Delta-like 1 is essential for postnatal arteriogenesis, Circ. Res. 100 (2007) 363–371.
[9] K. Takeshita, M. Satoh, M. Ii, M. Silver, F.P. Limbourg, Y. Mukai, et al., Critical role of endothelial Notch1 signaling in postnatal angiogenesis, Circ. Res. 100 (2007) 70–78.
[10] A. Duarte, M. Hirashima, R. Benedito, A. Trindade, P. Diniz, E. Bekman, et al., Dosage-sensitive requirement for mouse Dll4 in artery development, Genes Dev. 18 (2004) 2474–2478.
[11] L.T. Krebs, Y. Xue, C.R. Norton, J.R. Shutter, M. Maguire, J.P. Sundberg, et al., Notch signaling is essential for vascular morphogenesis in mice, Genes Dev. 14 (2000) 1343–1352.
[12] Y. Xue, X. Gao, C.E. Lindsell, C.R. Norton, B. Chang, C. Hicks, et al., Embryonic lethality and vascular defects in mice lacking the Notch ligand Jagged1, Hum. Mol. Genet. 8 (1999) 723–730.
[13] F.F. del Amo, D.E. Smith, P.J. Swiatek, M. Gendron-Maguire, R.J. Greenspan, A.P. McMahon, et al., Expression pattern of Motch, a mouse homolog of Drosophila Notch, suggests an important role in early postimplantation mouse development, Development. 115 (1992) 737–744.
[14] P.J. Swiatek, C.E. Lindsell, F.F. del Amo, G. Weinmaster, T. Gridley, Notch1 is essential for postimplantation development in mice, Genes Dev. 8 (1994) 707–719.
[15] N.W. Gale, M.G. Dominguez, I. Noguera, L. Pan, V. Hughes, D.M. Valenzuela, et al., Haploinsufficiency of delta-like 4 ligand results in embryonic lethality due to major defects in arterial and vascular development, Proc. Natl. Acad. Sci. USA. 101 (2004) 15949–15954.
[16] I. Dimova, R. Hlushchuk, A. Makanya, B. Styp-Rekowska, A. Ceausu, S. Flueckiger, et al., Inhibition of Notch signaling induces extensive intussusceptive neo-angiogenesis by recruitment of mononuclear cells, Angiogenesis. 16 (2013) 921–937.
[17] M. Hellström, L.-K. Phng, J.J. Hofmann, E. Wallgard, L. Coultas, P. Lindblom, et al., Dll4 signalling through Notch1 regulates formation of tip cells during angiogenesis, Nature. 445 (2007) 776–780.
[18] I.B. Lobov, R.A. Renard, N. Papadopoulos, N.W. Gale, G. Thurston, G.D. Yancopoulos, et al., Delta-like ligand 4 (Dll4) is induced by VEGF as a negative regulator of angiogenic sprouting, Proc. Natl. Acad. Sci. USA. 104 (2007) 3219–3224.
[19] S. Suchting, C. Freitas, F. le Noble, R. Benedito, C. Bréant, A. Duarte, et al., The Notch ligand Delta-like 4 negatively regulates endothelial tip cell formation and vessel branching, Proc. Natl. Acad. Sci. USA. 104 (2007) 3225–3230.
[20] R. Benedito, M. Hellström, Notch as a hub for signaling in angiogenesis, Exp. Cell Res. 319 (2013) 1281–1288.

[21] V. Caolo, N.M.S. van den Akker, S. Verbruggen, M.M.P.C. Donners, G. Swennen, H. Schulten, et al., Feed-forward Signaling by Membrane-bound Ligand Receptor Circuit: THE CASE OF NOTCH DELTA-LIKE 4 LIGAND IN ENDOTHELIAL CELLS, J. Biol. Chem. 285 (2010) 40681–40689.
[22] L.C. Napp, M. Augustynik, F. Paesler, K. Krishnasamy, J. Woiterski, A. Limbourg, et al., Extrinsic Notch ligand Delta-like 1 regulates tip cell selection and vascular branching morphogenesis, Circ. Res. 110 (2012) 530–535.
[23] C.M. Blaumueller, H. Qi, P. Zagouras, S. Artavanis-Tsakonas, Intracellular cleavage of Notch leads to a heterodimeric receptor on the plasma membrane, Cell. 90 (1997) 281–291.
[24] F. Logeat, C. Bessia, C. Brou, O. LeBail, S. Jarriault, N.G. Seidah, et al., The Notch1 receptor is cleaved constitutively by a furin-like convertase, Proc. Natl. Acad. Sci. USA. 95 (1998) 8108–8112.
[25] W.R. Gordon, D. Vardar-Ulu, S. L'heureux, T. Ashworth, M.J. Malecki, C. Sanchez-Irizarry, et al., Effects of S1 cleavage on the structure, surface export, and signaling activity of human Notch1 and Notch2, PLoS ONE. 4 (2009) e6613.
[26] E.C. Bozkulak, G. Weinmaster, Selective use of ADAM10 and ADAM17 in activation of Notch1 signaling, Mol. Cell. Biol. 29 (2009) 5679–5695.
[27] E.H. Schroeter, J.A. Kisslinger, R. Kopan, Notch-1 signalling requires ligand-induced proteolytic release of intracellular domain, Nature. 393 (1998) 382–386.
[28] G. van Tetering, P. van Diest, I. Verlaan, E. van der Wall, R. Kopan, M. Vooijs, Metalloprotease ADAM10 is required for Notch1 site 2 cleavage, J. Biol. Chem. 284 (2009) 31018–31027.
[29] B. De Strooper, W. Annaert, P. Cupers, P. Saftig, K. Craessaerts, J.S. Mumm, et al., A presenilin-1-dependent gamma-secretase-like protease mediates release of Notch intracellular domain, Nature. 398 (1999) 518–522.
[30] J.S. Mumm, E.H. Schroeter, M.T. Saxena, A. Griesemer, X. Tian, D.J. Pan, et al., A ligand-induced extracellular cleavage regulates gamma-secretase-like proteolytic activation of Notch1, Mol. Cell. 5 (2000) 197–206.
[31] S. Jarriault, C. Brou, F. Logeat, E.H. Schroeter, R. Kopan, A. Israël, Signalling downstream of activated mammalian Notch, Nature. 377 (1995) 355–358.
[32] M.M. Maier, M. Gessler, Comparative analysis of the human and mouse Hey1 promoter: Hey genes are new Notch target genes, Biochem. Biophys. Res. Commun. 275 (2000) 652–660.
[33] E. Lamar, G. Deblandre, D. Wettstein, V. Gawantka, N. Pollet, C. Niehrs, et al., Nrarp is a novel intracellular component of the Notch signaling pathway, Genes Dev. 15 (2001) 1885–1899.
[34] A.V. Morales, Y. Yasuda, D. Ish-Horowicz, Periodic Lunatic fringe expression is controlled during segmentation by a cyclic transcriptional enhancer responsive to notch signaling, Dev. Cell. 3 (2002) 63–74.
[35] H. Kato, T. Sakai, K. Tamura, S. Minoguchi, Y. Shirayoshi, Y. Hamada, et al., Functional conservation of mouse Notch receptor family members, FEBS Lett. 395 (1996) 221–224.
[36] C.-T. Ong, H.-T. Cheng, L.-W. Chang, T. Ohtsuka, R. Kageyama, G.D. Stormo, et al., Target selectivity of vertebrate notch proteins. Collaboration between discrete domains and CSL-binding site architecture determines activation probability, J. Biol. Chem. 281 (2006) 5106–5119.
[37] H. Uyttendaele, G. Marazzi, G. Wu, Q. Yan, D. Sassoon, J. Kitajewski, Notch4/int-3, a mammary proto-oncogene, is an endothelial cell-specific mammalian Notch gene, Development. 122 (1996) 2251–2259.
[38] C.J. Shawber, I. Das, E. Francisco, J. Kitajewski, Notch signaling in primary endothelial cells, Ann. N. Y. Acad. Sci. 995 (2003) 162–170.
[39] C.J. Shawber, Y. Funahashi, E. Francisco, M. Vorontchikhina, Y. Kitamura, S.A. Stowell, et al., Notch alters VEGF responsiveness in human and murine endothelial cells by direct

regulation of VEGFR-3 expression, J. Clin. Invest. 117 (2007) 3369–3382.
[40] T.R. Carlson, Y. Yan, X. Wu, M.T. Lam, G.L. Tang, L.J. Beverly, et al., Endothelial expression of constitutively active Notch4 elicits reversible arteriovenous malformations in adult mice, Proc. Natl. Acad. Sci. USA. 102 (2005) 9884–9889.
[41] H. Uyttendaele, J. Ho, J. Rossant, J. Kitajewski, Vascular patterning defects associated with expression of activated Notch4 in embryonic endothelium, Proc. Natl. Acad. Sci. USA. 98 (2001) 5643–5648.
[42] D. Miniati, E.B. Jelin, J. Ng, J. Wu, T.R. Carlson, X. Wu, et al., Constitutively active endothelial Notch4 causes lung arteriovenous shunts in mice, Am. J. Physiol. Lung Cell. Mol. Physiol. 298 (2010) L169–77.
[43] P.A. Murphy, M.T.Y. Lam, X. Wu, T.N. Kim, S.M. Vartanian, A.W. Bollen, et al., Endothelial Notch4 signaling induces hallmarks of brain arteriovenous malformations in mice, Proc. Natl. Acad. Sci. USA. 105 (2008) 10901–10906.
[44] M.J. Costa, X. Wu, H. Cuervo, R. Srinivasan, S.K. Bechis, E. Cheang, et al., Notch4 is required for tumor onset and perfusion, Vasc. Cell. 5 (2013) 7.
[45] A.G. Reaume, R.A. Conlon, R. Zirngibl, T.P. Yamaguchi, J. Rossant, Expression analysis of a Notch homologue in the mouse embryo, Dev. Biol. 154 (1992) 377–387.
[46] Y. Shirayoshi, Y. Yuasa, T. Suzuki, K. Sugaya, E. Kawase, T. Ikemura, et al., Proto-oncogene of int-3, a mouse Notch homologue, is expressed in endothelial cells during early embryogenesis, Genes Cells. 2 (1997) 213–224.
[47] N. Villa, L. Walker, C.E. Lindsell, J. Gasson, M.L. Iruela-Arispe, G. Weinmaster, Vascular expression of Notch pathway receptors and ligands is restricted to arterial vessels, Mech. Dev. 108 (2001) 161–164.
[48] K. Umesono, K.K. Murakami, C.C. Thompson, R.M. Evans, Direct repeats as selective response elements for the thyroid hormone, retinoic acid, and vitamin D3 receptors, Cell. 65 (1991) 1255–1266.
[49] G. Chapman, L. Liu, C. Sahlgren, C. Dahlqvist, U. Lendahl, High levels of Notch signaling down-regulate Numb and Numblike, J. Cell Biol. 175 (2006) 535–540.
[50] S. Kredel, F. Oswald, K. Nienhaus, K. Deuschle, C. Röcker, M. Wolff, et al., mRuby, a bright monomeric red fluorescent protein for labeling of subcellular structures, PLoS ONE. 4 (2009) e4391.
[51] D.H. Pham, P.A.B. Moretti, G.J. Goodall, S.M. Pitson, Attenuation of leakiness in doxycycline-inducible expression via incorporation of 3' AU-rich mRNA destabilizing elements, BioTechniques. 45 (2008) 155–162.
[52] M.T. Saxena, E.H. Schroeter, J.S. Mumm, R. Kopan, Murine notch homologs (N1-4) undergo presenilin-dependent proteolysis, J. Biol. Chem. 276 (2001) 40268–40273.
[53] H. Karlström, A. Bergman, U. Lendahl, J. Näslund, J. Lundkvist, A sensitive and quantitative assay for measuring cleavage of presenilin substrates, J. Biol. Chem. 277 (2002) 6763–6766.
[54] H. Kato, Y. Taniguchi, H. Kurooka, S. Minoguchi, T. Sakai, S. Nomura-Okazaki, et al., Involvement of RBP-J in biological functions of mouse Notch1 and its derivatives, Development. 124 (1997) 4133–4141.
[55] T. Nishiyama, K. Mishima, F. Ide, K. Yamada, K. Obara, A. Sato, et al., Functional Analysis of an Established Mouse Vascular Endothelial Cell Line, J. Vasc. Res. 44 (2007) 138–148.
[56] D.B. Sparrow, G. Chapman, M.A. Wouters, N.V. Whittock, S. Ellard, D. Fatkin, et al., Mutation of the LUNATIC FRINGE gene in humans causes spondylocostal dysostosis with a severe vertebral phenotype, Am. J. Hum. Genet. 78 (2006) 28–37.
[57] G.F. Hoyne, G. Chapman, Y. Sontani, S.E. Pursglove, S.L. Dunwoodie, A cell autonomous role for the Notch ligand Delta-like 3 in αβ T-cell development, Immunol. Cell Biol. 89 (2011) 696–705.
[58] G. Chapman, D.B. Sparrow, E. Kremmer, S.L. Dunwoodie, Notch inhibition by the ligand

Delta-Like 3 defines the mechanism of abnormal vertebral segmentation in spondylocostal dysostosis, Hum. Mol. Genet. 20 (2011) 905–916.
[59] N.D. Borson, W.L. Salo, L.R. Drewes, A lock-docking oligo(dT) primer for 5“ and 3” RACE PCR, PCR Methods Appl. 2 (1992) 144–148.
[60] E. Scotto-Lavino, G. Du, M.A. Frohman, 3' end cDNA amplification using classic RACE, Nat. Protoc. 1 (2006) 2742–2745.
[61] T. Brown, K. Mackey, Analysis of RNA by northern and slot-blot hybridization, Curr Protoc Neurosci. Chapter 5 (2001) Unit 5.17.
[62] S.L. Dunwoodie, D. Henrique, S.M. Harrison, R.S. Beddington, Mouse Dll3: a novel divergent Delta gene which may complement the function of other Delta homologues during early pattern formation in the mouse embryo, Development. 124 (1997) 3065–3076.
[63] M.E. Seaman, S.M. Peirce, K. Kelly, Rapid Analysis of Vessel Elements (RAVE): A Tool for Studying Physiologic, Pathologic and Tumor Angiogenesis, PLoS ONE. 6 (2011) e20807.
[64] L.E. Maquat, Nonsense-mediated mRNA decay: splicing, translation and mRNP dynamics, Nat. Rev. Mol. Cell Biol. 5 (2004) 89–99.
[65] S. Claxton, M. Fruttiger, Periodic Delta-like 4 expression in developing retinal arteries, Gene Expr. Patterns. 5 (2004) 123–127.
[66] Y. Funahashi, S.L. Hernandez, I. Das, A. Ahn, J. Huang, M. Vorontchikhina, et al., A notch1 ectodomain construct inhibits endothelial notch signaling, tumor growth, and angiogenesis, Cancer Res. 68 (2008) 4727–4735.
[67] U.B. Pajvani, L. Qiang, T. Kangsamaksin, J. Kitajewski, H.N. Ginsberg, D. Accili, Inhibition of Notch uncouples Akt activation from hepatic lipid accumulation by decreasing mTorc1 stability, Nat. Med. 19 (2013) 1054–1060.
[68] S.L. Hernandez, D. Banerjee, A. Garcia, T. Kangsamaksin, W.-Y. Cheng, D. Anastassiou, et al., Notch and VEGF pathways play distinct but complementary roles in tumor angiogenesis, Vasc. Cell. 5 (2013) 17.
[69] M.D. Rand, L.M. Grimm, S. Artavanis-Tsakonas, V. Patriub, S.C. Blacklow, J. Sklar, et al., Calcium depletion dissociates and activates heterodimeric notch receptors, Mol. Cell. Biol. 20 (2000) 1825–1835.
[70] R. Kopan, J.S. Nye, H. Weintraub, The intracellular domain of mouse Notch: a constitutively activated repressor of myogenesis directed at the basic helix-loop-helix region of MyoD, Development. 120 (1994) 2385–2396.
[71] G. Bush, G. diSibio, A. Miyamoto, J.B. Denault, R. Leduc, G. Weinmaster, Ligand-induced signaling in the absence of furin processing of Notch1, Dev. Biol. 229 (2001) 494–502.
[72] M.I. Dorrell, M. Friedlander, Mechanisms of endothelial cell guidance and vascular patterning in the developing mouse retina, Prog. Retin. Eye Res. 25 (2006) 277–295.
[73] M. Fruttiger, Development of the retinal vasculature, Angiogenesis. 10 (2007) 77–88.
[74] M. Aste-Amézaga, N. Zhang, J.E. Lineberger, B.A. Arnold, T.J. Toner, M. Gu, et al., Characterization of Notch1 antibodies that inhibit signaling of both normal and mutated Notch1 receptors, PLoS ONE. 5 (2010) e9094.
[75] W.R. Gordon, D. Vardar-Ulu, G. Histen, C. Sanchez-Irizarry, J.C. Aster, S.C. Blacklow, Structural basis for autoinhibition of Notch, Nat. Struct. Mol. Biol. 14 (2007) 295–300.
[76] H. Uyttendaele, V. Closson, G. Wu, F. Roux, G. Weinmaster, J. Kitajewski, Notch4 and Jagged-1 induce microvessel differentiation of rat brain endothelial cells, Microvasc. Res. 60 (2000) 91–103.
[77] J.C. Aster, N. Bodnar, L. Xu, F. Karnell, J.M. Milholland, I. Maillard, et al., Notch ankyrin repeat domain variation influences leukemogenesis and Myc transactivation, PLoS ONE. 6 (2011) e25645.
[78] D. del Álamo, H. Rouault, F. Schweisguth, Mechanism and significance of cis-inhibition in Notch signalling, Curr. Biol. 21 (2011) R40–7.

[79] K. Sakamoto, O. Ohara, M. Takagi, S. Takeda, K.-I. Katsube, Intracellular cell-autonomous association of Notch and its ligands: a novel mechanism of Notch signal modification, Dev. Biol. 241 (2002) 313–326.
[80] K. Sakamoto, W.S. Chao, K.-I. Katsube, A. Yamaguchi, Distinct roles of EGF repeats for the Notch signaling system, Exp. Cell Res. 302 (2005) 281–291.
[81] M. Vooijs, E.H. Schroeter, Y. Pan, M. Blandford, R. Kopan, Ectodomain shedding and intramembrane cleavage of mammalian Notch proteins is not regulated through oligomerization, J. Biol. Chem. 279 (2004) 50864–50873.
[82] P. Chastagner, A. Israël, C. Brou, AIP4/Itch regulates Notch receptor degradation in the absence of ligand, PLoS ONE. 3 (2008) e2735.
[83] M.A. McGill, S.E. Dho, G. Weinmaster, C.J. McGlade, Numb regulates post-endocytic trafficking and degradation of Notch1, J. Biol. Chem. 284 (2009) 26427–26438.
[84] L. Li, G.M. Huang, A.B. Banta, Y. Deng, T. Smith, P. Dong, et al., Cloning, characterization, and the complete 56.8-kilobase DNA sequence of the human NOTCH4 gene, Genomics. 51 (1998) 45–58.
[85] L.-K. Phng, M. Potente, J.D. Leslie, J. Babbage, D. Nyqvist, I. Lobov, et al., Nrarp coordinates endothelial Notch and Wnt signaling to control vessel density in angiogenesis, Dev. Cell. 16 (2009) 70–82.
[86] P.A. Murphy, T.N. Kim, G. Lu, A.W. Bollen, C.B. Schaffer, R.A. Wang, Notch4 normalization reduces blood vessel size in arteriovenous malformations, Sci. Transl. Med. 4 (2012) 1–11.

Figure Legends

Figure 1. The *Notch4*^{d1} allele overexpresses a truncated *Notch4* transcript *in vivo*.
(A) Schematic representation of the *Notch4* and *Notch4*^{d1} alleles. The position of PCR products and probes are indicated by lines. (B) Expression of transcripts derived from exons 1-5 (ex1/5 probe) in *Notch4*$^{+/+}$ and *Notch4*$^{d1/d1}$ E10.5 embryos shown by wholemount RNA *in situ* hybridisation. Scale bar: 1.7 mm for whole embryos (left) and 1 mm for tail region (right) (C) Confirmation of the *Notch4* locus structure in the *Notch4*^{d1} allele by PCR from genomic DNA. The PCR products are 313 bp (ex22); 469 bp (ex21/neo); 518 bp (neo); 735 bp (neo/ex25). (D) Detection of *Notch4*^{d1} transcripts containing sequences 5' of the *neo* cassette insertion in neonatal lung RNA by RT-PCR. The PCR products are 313 bp (ex22); 518 bp (neo); 199 bp (ex1/3); 160 bp (ex15/16). (E) Detection of transcripts containing *Notch4* exons 1-5 in lung from *Notch4*$^{+/+}$, *Notch4*$^{+/d1}$ and *Notch4*$^{d1/d1}$ neonates by northern blot analysis. White and black arrows indicate the *Notch4 and Notch4*^{d1} transcripts, respectively. Molecular weights (kb) are shown on the left. (F) Quantitation of transcripts detected by northern blot containing exons 1-5 in lung from *Notch4*$^{+/+}$, *Notch4*$^{+/d1}$ and *Notch4*$^{d1/d1}$ neonates. Average expression and standard error of the mean relative to 28S rRNA, n=3 for each genotype. Data was tested for statistical significance as described in the experimental procedures. *$p < 0.05$. Exons (ex). Neomycin (neo).

Figure 2. The *Notch4*^{d1} allele overexpresses a truncated NOTCH4 protein *in vivo*.
(A-C) Wholemount immunofluorescent detection of NOTCH4 (red) in wildtype retinas at P5 in arteries (A), veins (B) and at the vascular front (C). Vasculature was labelled with Alexa-488 conjugated Isolectin B4 (IB4; green). (D,E) Wholemount immunofluorescent detection of NOTCH4 (red) in *Notch4*$^{+/+}$, *Notch4*$^{+/d1}$ and *Notch4*$^{d1/d1}$ P5 retinas. (D) Arterial and (E) tip cell staining for NOTCH4 in IB4-positive endothelial cells (green). Scale bar: 100 μm (A-C) and 20 μm (D, E).

Figure 3. NOTCH4 inhibits NOTCH1 signalling in cultured cells.
(A) Notch signal transduction assay following coculture of ligand expressing (DLL4) or control cells, with NIH3T3 cells transfected with various Notch receptor cDNAs (Notch4, Notch4d1, Notch1) and a Notch responsive luciferase reporter. (B) Notch signal transduction assay in NIH3T3 cells transfected with increasing amounts (25, 50, 100, 200 ng per well) of either NOTCH1ΔE or NOTCH4ΔE and a Notch responsive luciferase reporter. (C) Signalling via chimaeric Notch receptors cocultured with JAG1 expressing cells. NIH3T3 cells were transfected with Notch chimaeric constructs and a Notch responsive reporter and signalling upon JAG1 coculture was normalised to coculture with control cells. Diagram indicates chimaeric Notch receptor constructs containing sequences derived from NOTCH1 (black) and NOTCH4 (white). EGF-epidermal growth factor-like domain, LNR-Lin-12/Notch repeat, TM-transmembrane domain, ANK-Ankyrin repeat, AscI-AscI restriction enzyme site. (D) Notch signal transduction assay following coculture of ligand-expressing (DLL4) or control cells, with NIH3T3 cells transfected with NOTCH1 (25 ng), increasing amounts of NOTCH4ΔE (25, 50, 100, 200 ng) and a Notch responsive luciferase reporter. (A, B, and D) The columns represent the average relative luciferase activity and standard error of the mean of three independent experiments. Data were tested for statistical significance as described in the experimental procedures. *$p < 0.05$, **$p < 0.01$. (E) Comparison of C2C12 myoblast differentiation in control cells and those expressing Notch4 or Notch4d1 cDNA. Differentiated muscle cells were identified by reactivity to the pan-sarcomeric myosin antibody MF20 (green). Nuclei are stained with TO-PRO 3 (red). NotchΔE constructs include the PEST sequence and span the membrane but lack the LNR, HD and EGF repeats. Scale bar: 200 μm.

Figure 4. NOTCH4 interacts with NOTCH1 and alters its subcellular localisation.
(A) Co-immunoprecipitation of stably transfected HA-tagged NOTCH1 in C2C12 cells with transiently transfected FLAG-tagged (FL) NOTCH4 or NOTCH4d1. Proteins were immunoprecipitated with either mouse anti-FLAG (FL, lanes 5, 7 and 9) or non-specific mouse IgG (Ig, lanes 6 and 8) and immunoblotted to detect NOTCH1HA with anti-HA. Full-length (unprocessed: white arrow) NOTCH1 precipitates with NOTCH4 (lane 7) and NOTCH4d1 (lane 9)

using anti-HA while heterodimeric NOTCH1 (black arrow) does not. IP (immunoprecipitation). WB (western blot). L (lysate). (B) Still images from live-cell imaging (see movie 1) of cells expressing NOTCH1-GFP (green) and induced to express NOTCH4-Ruby (red). Time (minutes) post induction of NOTCH4-Ruby is indicated on the right. Cell expressing NOTCH1-GFP before induction of NOTCH4-Ruby expression (asterisk). Colocalisation of NOTCH1-GFP and NOTCH4-Ruby is indicated by the arrow head. Scale bar: 20 μm. (C) Coexpression of NOTCH4 with NOTCH1 increases the amount of full-length NOTCH1. NIH3T3 cells stably expressing myc-tagged NOTCH1 were transfected with increasing quantities of HA-tagged NOTCH4 (100, 200, 400, 800 ng) and immunoblotted to detect NOTCH1 (anti-myc), NOTCH4 (anti-HA) and β-actin (anti-ACTB) White arrow (full-length NOTCH1). Black arrow (processed, heterodimeric NOTCH1). (D) Levels of full-length NOTCH1 (white bars) and NOTCH1 heterodimer (black bars) in (C) in the presence of increasing quantities of HA-tagged NOTCH4. Values are expressed relative to levels of NOTCH1 in the absence of NOTCH4HA.

Figure 5. Structure and confirmation of the *Notch4*$^{tm1(KOMP)Vlcg}$ *(Notch4*$^{-}$*)* allele.
(A) Diagram of the *Notch4* allele and the *LacZ/neo* cassette inserted between the start and stop codons of the *Notch4* gene. Lines indicate the positions of PCR products. (B) PCR of genomic DNA from *Notch4*$^{+/+}$*, Notch4*$^{+/-}$ and *Notch4*$^{-/-}$ mice amplifying regions indicated in (A). The PCR products are 313 bp (ex22); 532 bp (5'/LacZ); 544 bp (neo/3'). (C-F) Wholemount β-galactosidase staining of *Notch4*$^{+/+}$ (C) and *Notch4*$^{d1/d1}$ E10.5 embryos (D-F). Scale bar: 500 μm (C and D) and 836 μm (E and F).

Figure 6. The *Notch4*^{d1} and *Notch4*$^{-}$ alleles affect formation of the retinal vasculature.
(A, B) Wholemount immunofluorescence staining for the endothelial marker PECAM1 (red) and smooth muscle marker ACTA2 (green) of the retina of P5 *Notch4*$^{+/+}$, *Notch4*$^{+/d1}$ and *Notch4*$^{d1/d1}$ littermates (A) and *Notch4*$^{+/+}$, *Notch4*$^{+/-}$ and *Notch4*$^{-/-}$ littermates (B). (C, F) Measurements of the retinal vascular area in *Notch4*$^{+/+}$, *Notch4*$^{+/d1}$ and *Notch4*$^{d1/d1}$ (C) and *Notch4*$^{+/+}$, *Notch4*$^{+/-}$ and *Notch4*$^{-/-}$ mice (F). (D, G) Total vessel length of *Notch4*$^{+/+}$, *Notch4*$^{+/d1}$ and *Notch4*$^{d1/d1}$ (D) and *Notch4*$^{+/+}$, *Notch4*$^{+/-}$ and *Notch4*$^{-/-}$ retinas (G). (E, H) Graphs of vessel length density in *Notch4*$^{+/+}$, *Notch4*$^{+/d1}$ and *Notch4*$^{d1/d1}$ (E) and *Notch4*$^{+/+}$, *Notch4*$^{+/-}$ and *Notch4*$^{-/-}$ retinas (H). Measurements were normalised to the mean of the heterozygotes in each litter. Red data points correspond to littermates of each genotype shown in A. and B. These data were tested for statistical significance as described in the experimental procedures, *$p < 0.05$, **$p < 0.01$. Scale bar: 500 μm.

movie 1. NOTCH4 alters the subcellular localisation of NOTCH1.

Live-cell imaging of C2C12 cells expressing NOTCH1-GFP (green) and induced to express NOTCH4-Ruby (red). Time (minutes) post induction of NOTCH4-Ruby is indicated.

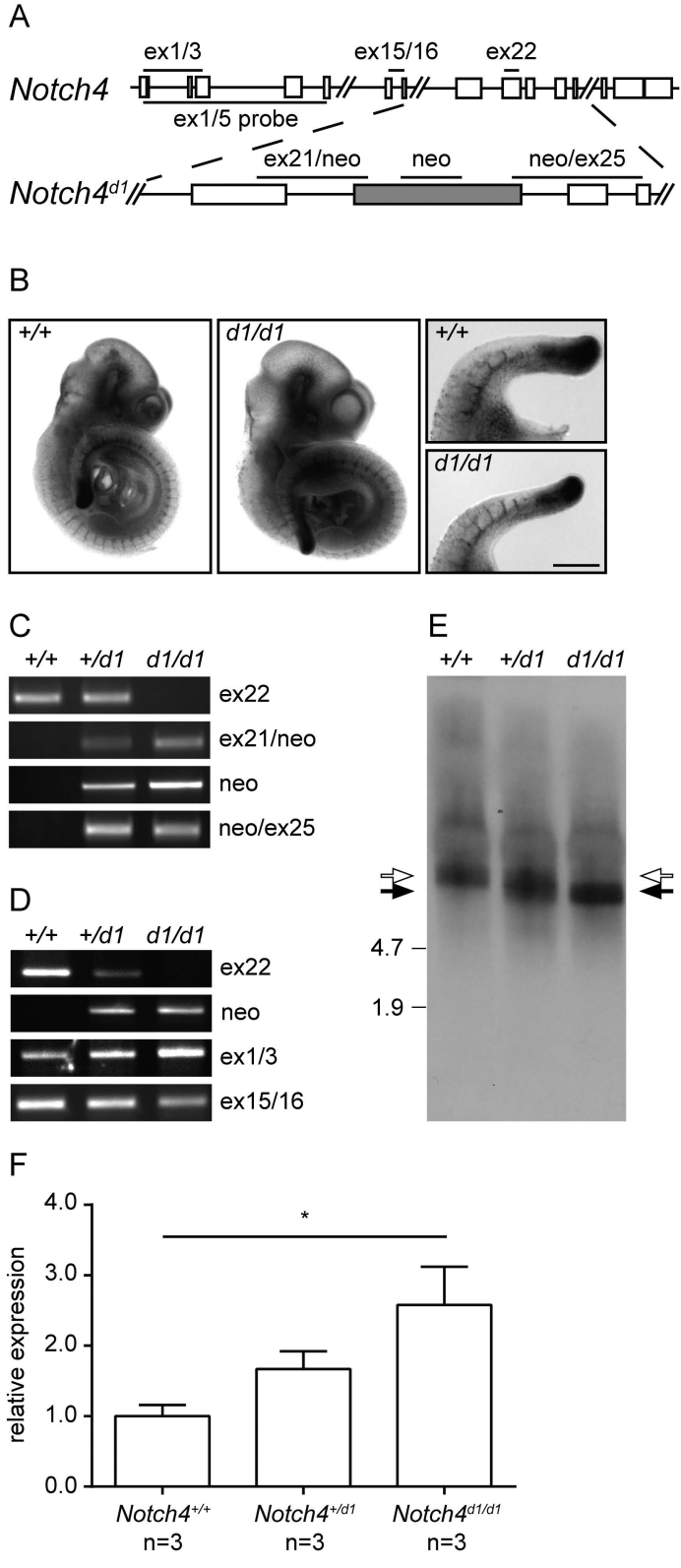
A
ex1/3
ex15/16
ex22
Notch4
ex1/5 probe
ex21/neo
neo
neo/ex25
Notch4d1
B
+/+
d1/d1
+/+
d1/d1
C
+/+
+/d1
d1/d1
ex22
ex21/neo
neo
neo/ex25
D
+/+
+/d1
d1/d1
ex22
neo
ex1/3
ex15/16
E
+/+
+/d1
d1/d1
4.7
1.9
F
4.0
3.0
2.0
1.0
0.0
relative expression
*
Notch4+/+
n=3
Notch4+/d1
n=3
Notch4d1/d1
n=3

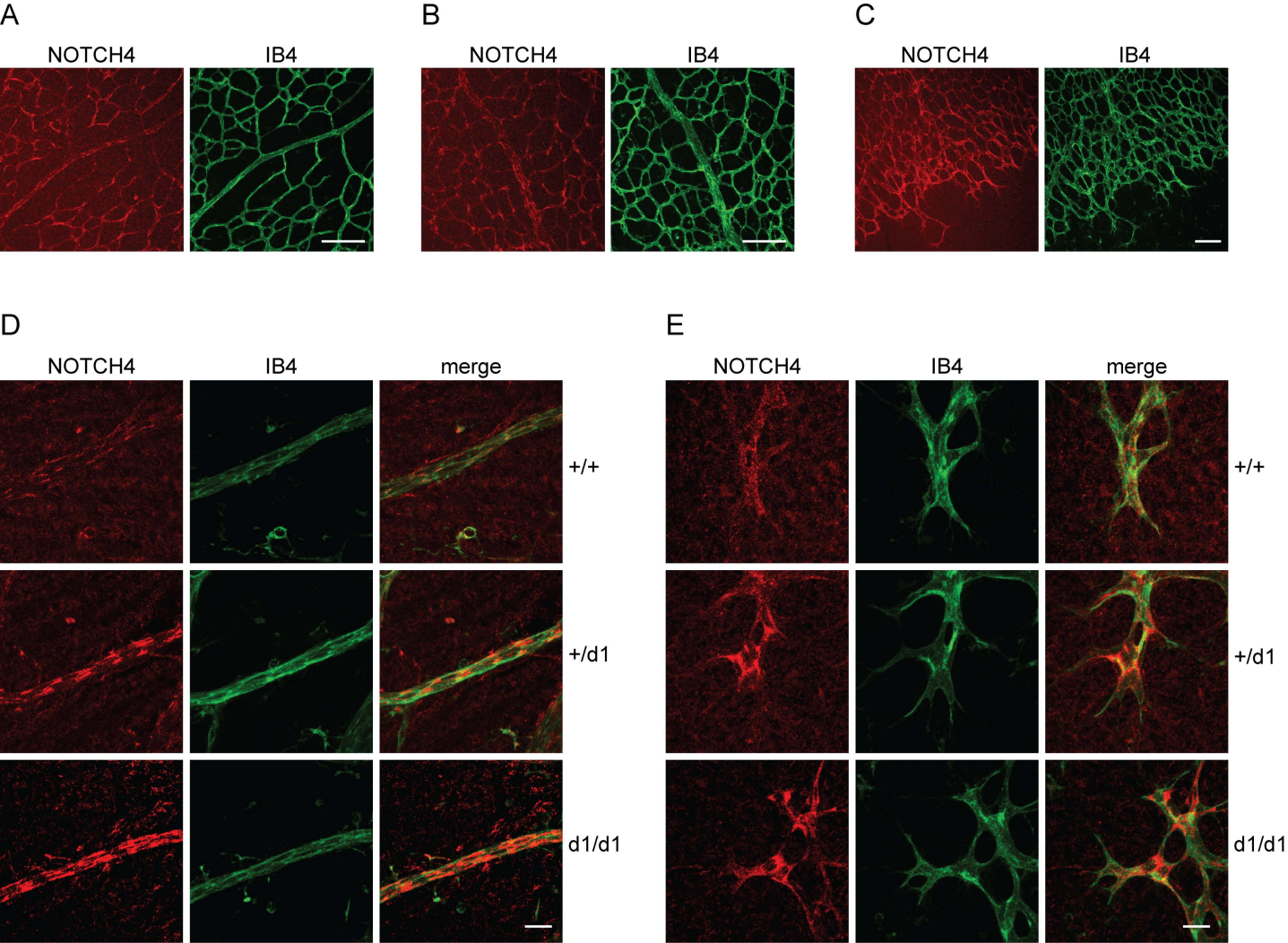
A
NOTCH4
IB4
B
NOTCH4
IB4
C
NOTCH4
IB4
D
NOTCH4
IB4
merge
+/+
+/d1
d1/d1
E
NOTCH4
IB4
merge
+/+
+/d1
d1/d1

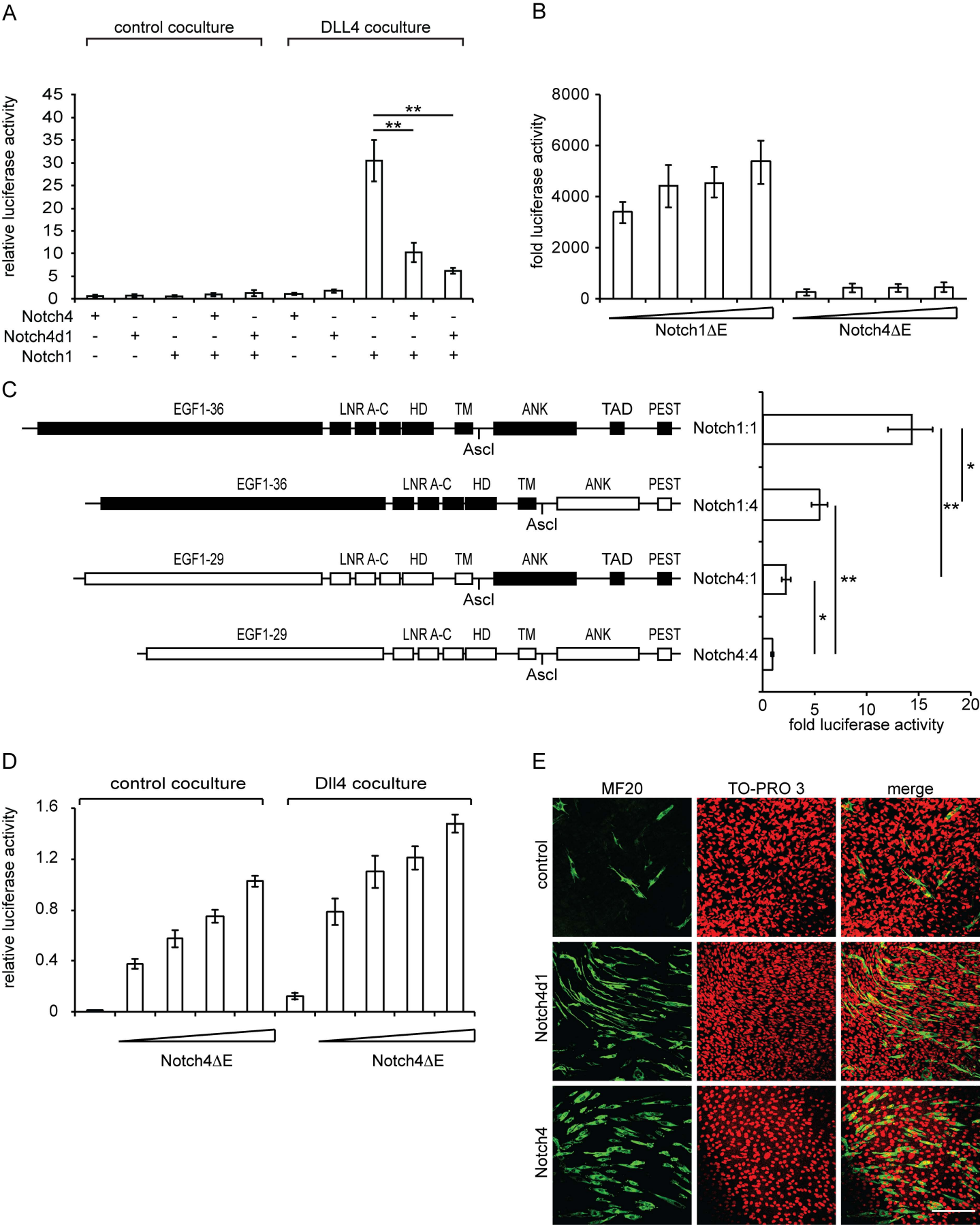
A
control coculture
DLL4 coculture
relative luciferase activity
45
40
35
30
25
20
15
10
5
0
**
**
Notch4 + - - + - + - - + -
Notch4d1 - + - - + - + - - +
Notch1 - - + + + - - + + +
B
fold luciferase activity
8000
6000
4000
2000
0
Notch1ΔE
Notch4ΔE
C
EGF1-36
LNR A-C
HD
TM
ANK
TAD
PEST
AscI
EGF1-29
Notch1:1
Notch1:4
Notch4:1
Notch4:4
*
**
**
*
0
5
10
15
20
fold luciferase activity
D
control coculture
Dll4 coculture
relative luciferase activity
1.6
1.2
0.8
0.4
0
Notch4ΔE
Notch4ΔE
E
MF20
TO-PRO 3
merge
control
Notch4d1
Notch4

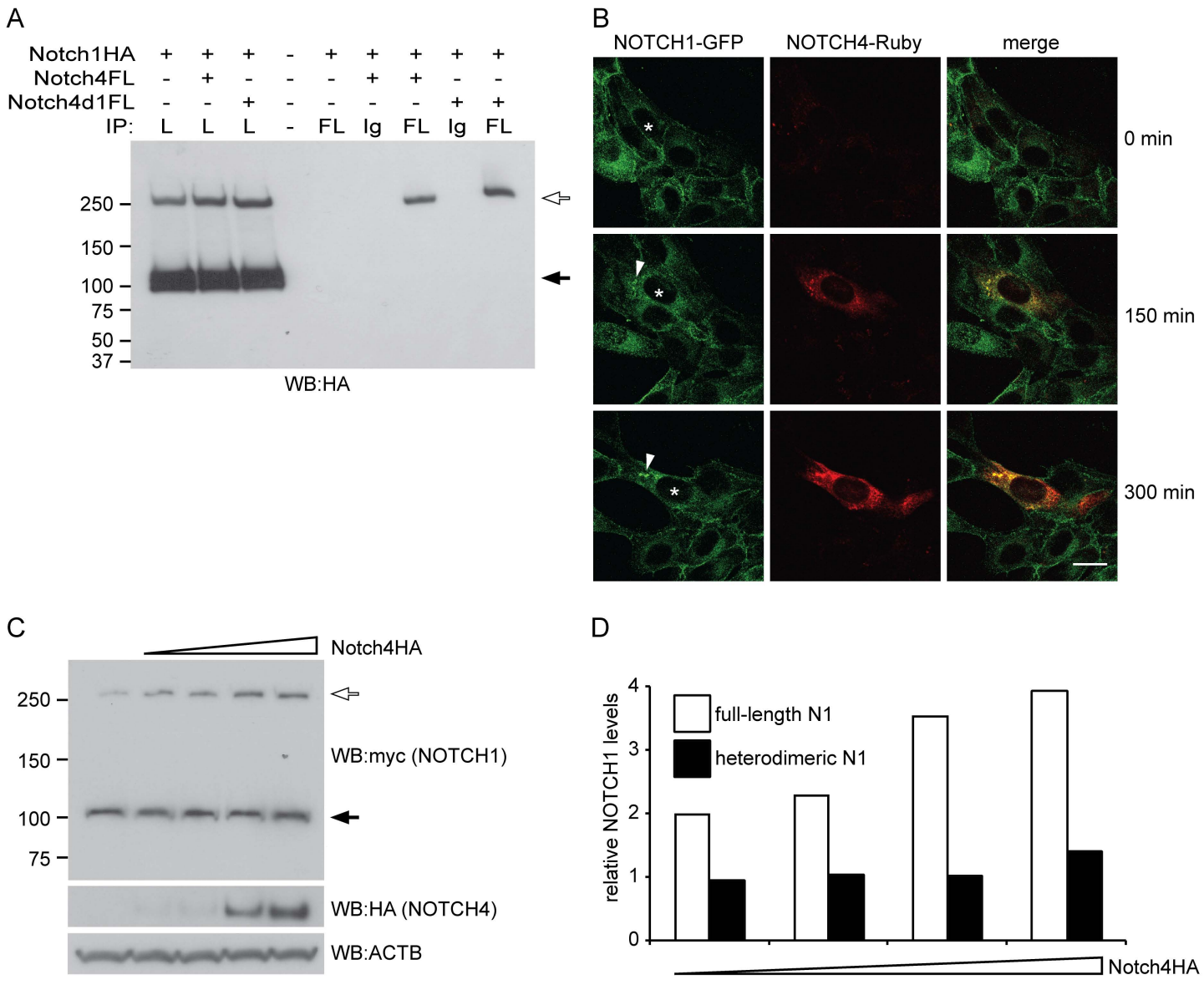
A
Notch1HA + + + - + + + + +
Notch4FL - + - - - + + - -
Notch4d1FL - - + - - - - + +
IP: L L L - FL Ig FL Ig FL
250
150
100
75
50
37
WB:HA
B
NOTCH1-GFP
NOTCH4-Ruby
merge
0 min
150 min
300 min
C
Notch4HA
250
150
100
75
WB:myc (NOTCH1)
WB:HA (NOTCH4)
WB:ACTB
D
relative NOTCH1 levels
full-length N1
heterodimeric N1
0
1
2
3
4
Notch4HA

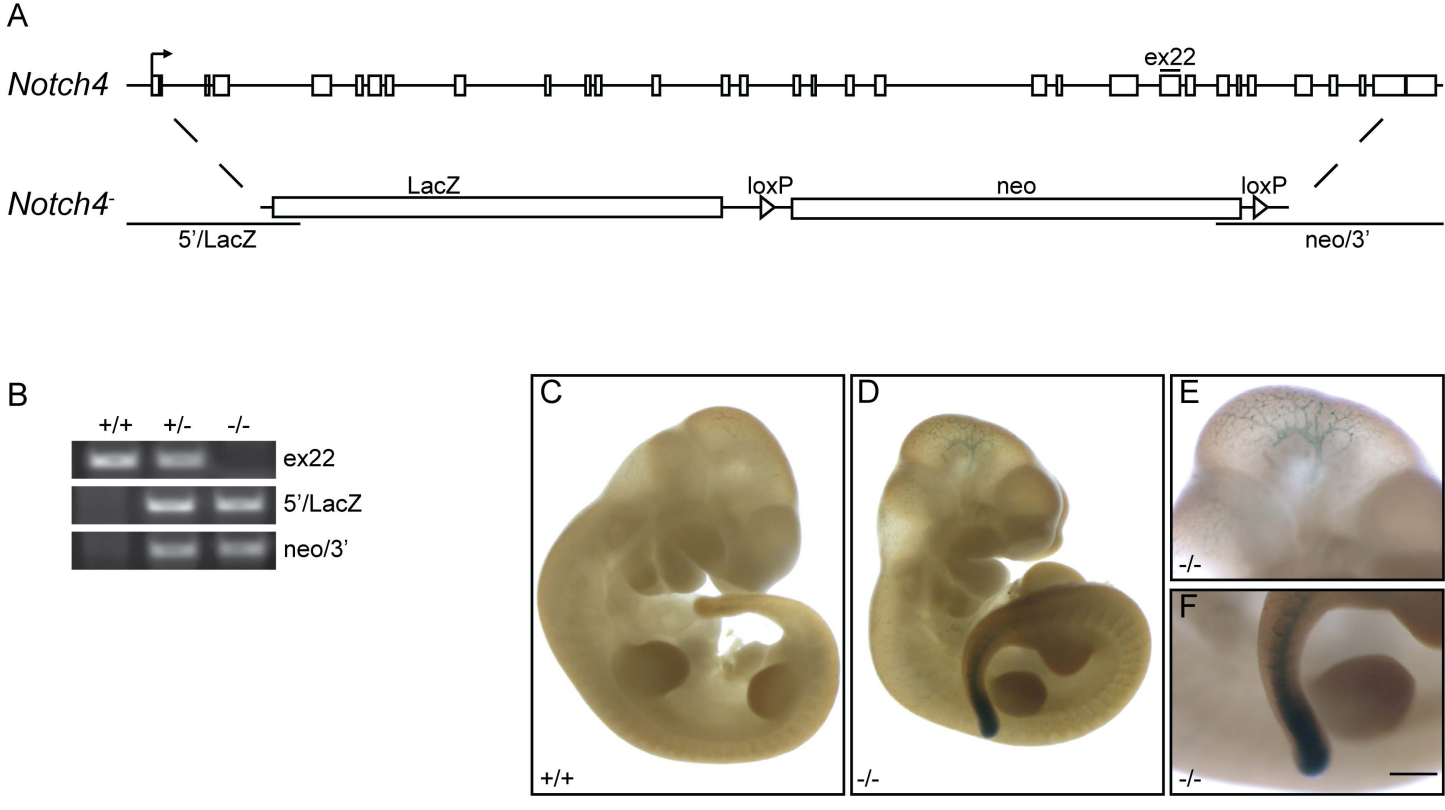
A
Notch4
ex22
Notch4-
LacZ
loxP
neo
loxP
5'/LacZ
neo/3'
B
+/+
+/-
-/-
ex22
5'/LacZ
neo/3'
C
+/+
D
-/-
E
-/-
F
-/-

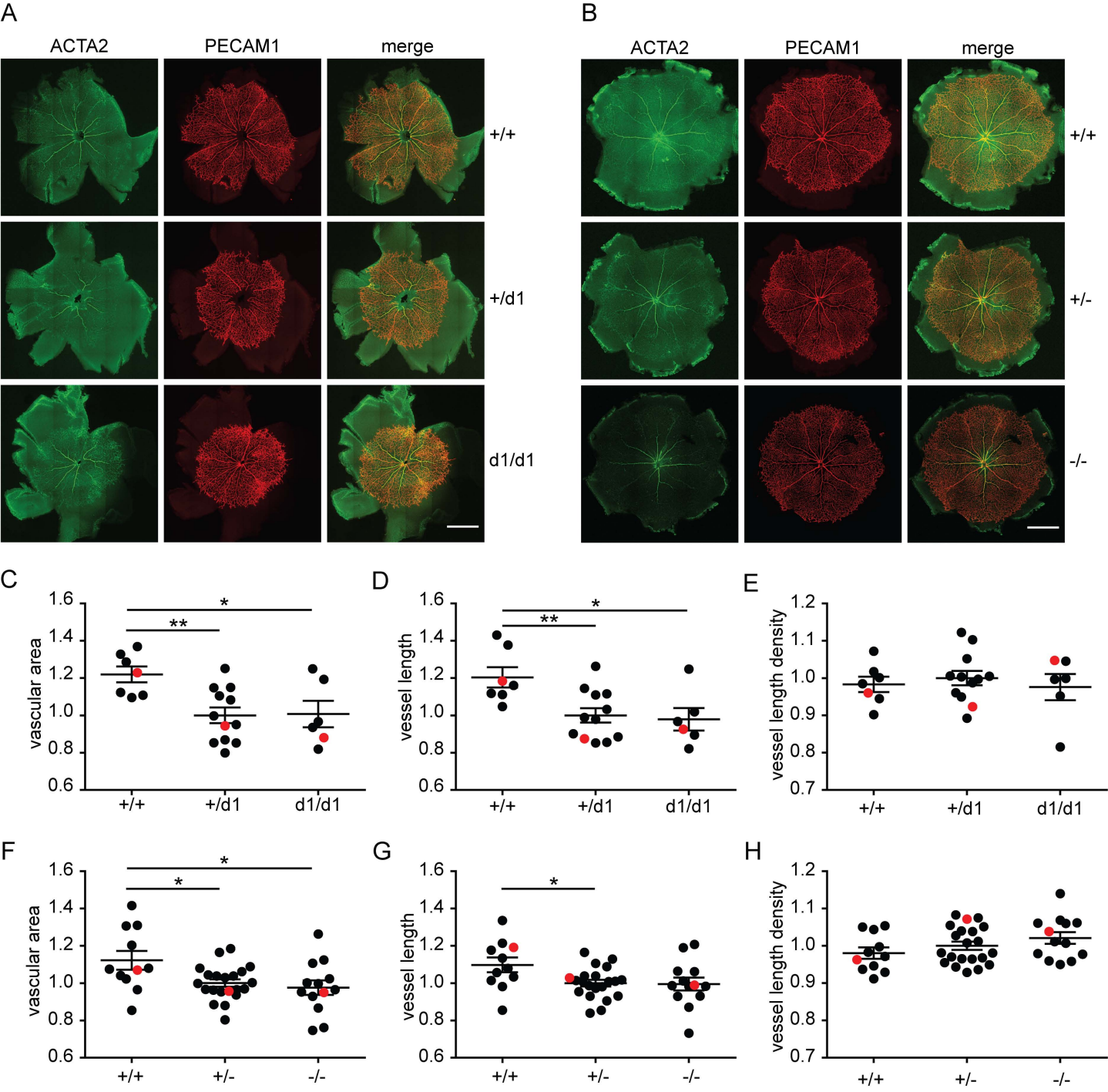
A
ACTA2
PECAM1
merge
+/+
+/d1
d1/d1
B
ACTA2
PECAM1
merge
+/+
+/-
-/-
C
vascular area
1.6
1.4
1.2
1.0
0.8
0.6
*
**
+/+
+/d1
d1/d1
D
vessel length
1.6
1.4
1.2
1.0
0.8
0.6
*
**
+/+
+/d1
d1/d1
E
vessel length density
1.2
1.1
1.0
0.9
0.8
0.7
+/+
+/d1
d1/d1
F
vascular area
1.6
1.4
1.2
1.0
0.8
0.6
*
*
+/+
+/-
-/-
G
vessel length
1.6
1.4
1.2
1.0
0.8
0.6
*
+/+
+/-
-/-
H
vessel length density
1.2
1.1
1.0
0.9
0.8
0.7
+/+
+/-
-/-

A

```
CCA GGA GGA GAC TGG GAT GGA GGG GAC TGT TCC CTG GGG GTC CCA GAC CCC
 P   G   G   D   W   D   G   G   D   C   S   L   G   V   P   D   P
TGG AAG GGC TGT CCC CCG CAT TCC CAG TGC TGG CTT CTG TTC CGG GAC GGA
 K   W   G   C   P   P   H   S   Q   C   W   L   L   F   R   D   G
CGG TGT CAC CCG CAG TGT GAC TCT GAG GAG TGT CTC TTT GAT GGC TAC GAC
 R   C   H   P   Q   C   D   S   E   E   C   L   F   D   G   Y   D
TGT GAA ATC CCT CTA TGC ATC TCG CGT CGT GCA GGA CGT GAC AAA TGG AAG
 C   E   I   P   L   C   I   S   R   R   A   G   R   D   K   W   K
TAG CACGTCTCACTAGTCTCGTGCAGATGGACAGCACCGCTGAGCAATGGAAGCGGCCAATATGGG
 *
ATCGGCCATTGAACAAGATGGATTGCACGCAGGTTCTCCGGCCGCTTGGGTGGAGAGGCTATTCGGCT
ATGACGGCACAACAGACAATCGGCTGCTCTGATGCCGCCGTGTTCCGGCTGTCAGCGCAGGGGCGCCC
GGTTCTTTTTGTCAAGACCGACCTGTCCGGTGCCCTGAATGAACTGCAGGACGAGGCAGCGCGGCTAT
CGTGGCTGGCCACGACGGGCGTTCCTTGCGCAGCTGTGCTCGACGTTGTCACTGAAGCGGGAAGGGAC
TGGCTGCTATTGGGCGAAGTGCCGGGGCAGGATCTCCTGTCATCTCACCTTGCTCCTGCCGAGAAAGT
ATCCATCATGGCTGATGCAATGCGGCGGCTGCATACGCTTGATCCGGCTACCTGCCCATTCGACCACC
AAGCGAAACATCGCATCGAGCGAGCACGTACTCGGATGGAAGCCGGTCTTGTCGATCAGGATGATCTG
GACGAAGAGCATCAGGGGCTCGCGCCAGCCGAACTGTTCGCCAGGCTCAAGGCGCGCATGCCCGACGG
CGATGATCTCGTCGTGACCCATGGCGATGCCTGCTTGCCGAATATCATGGTGGAAAATGGCCGCTTTT
CTGGATTCATCGACTGTGGCCGGCTGGGTGTGGCGGACCGCTATCAGGACATAGCGTTGGCTACCCGT
GATATTGCTGAAGAGCTTGGCGGCGAATGGGCTGACCGCTTCCTCGTGCTTTACGGTATCGCCGCTCC
CGACTCGCAGCGCATCGCCTTCTATCGCCTTCTTGACGAGTTCTTCTGAGGGGATCAATTCTCTAGAG
CTCGCTGATCAGCCTCGACTGTGCCTTCTAGTTGCCAGCCATCTGTTGTTTGCCCCTCCCCCGTGCCT
TCCTTGACCCTGGAAGGTGCCACTCCCACTGTCCTTTCCT AATAAA ATGAGGAAATTGCATCGC AAAA
AAAAAAAAAAAA
```

B

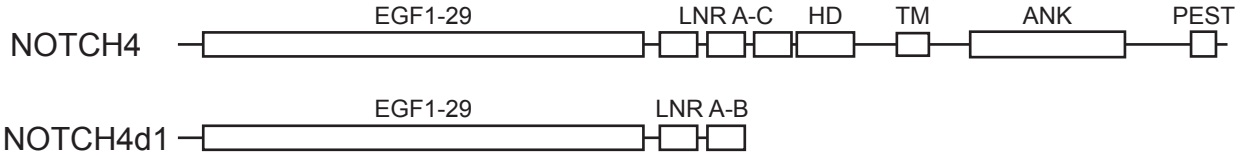

Supplemental Figure 1. The transcript and predicted protein expressed from the *Notch4*^{d1} allele. (A) The 3' end of exon 21 of *Notch4* (red) was fused to the first novel exon (blue) within the *neo* cassette encoding 10 nonsense amino acids before a stop codon (*). The polyadenylation consensus signal and poly(A) tail of the *neo* cassette are in bold and underlined, respectively. (B) Schematic representation of the proteins encoded by the *Notch4* alleles. Top: NOTCH4 consists of extracellular and intracellular domains separated by a transmembrane (TM) domain. The extracellular domain consists of 29 EGF-like repeats (EGF1-29) and three Lin12-Notch repeats (LNR A-C). The intracellular domain consists of Ankyrin repeats (ANK) and PEST sequence. Bottom: The predicted NOTCH4d1 protein encoded by the *Notch4*^{d1} derived transcript lacks domains C-terminal to LNR-B.

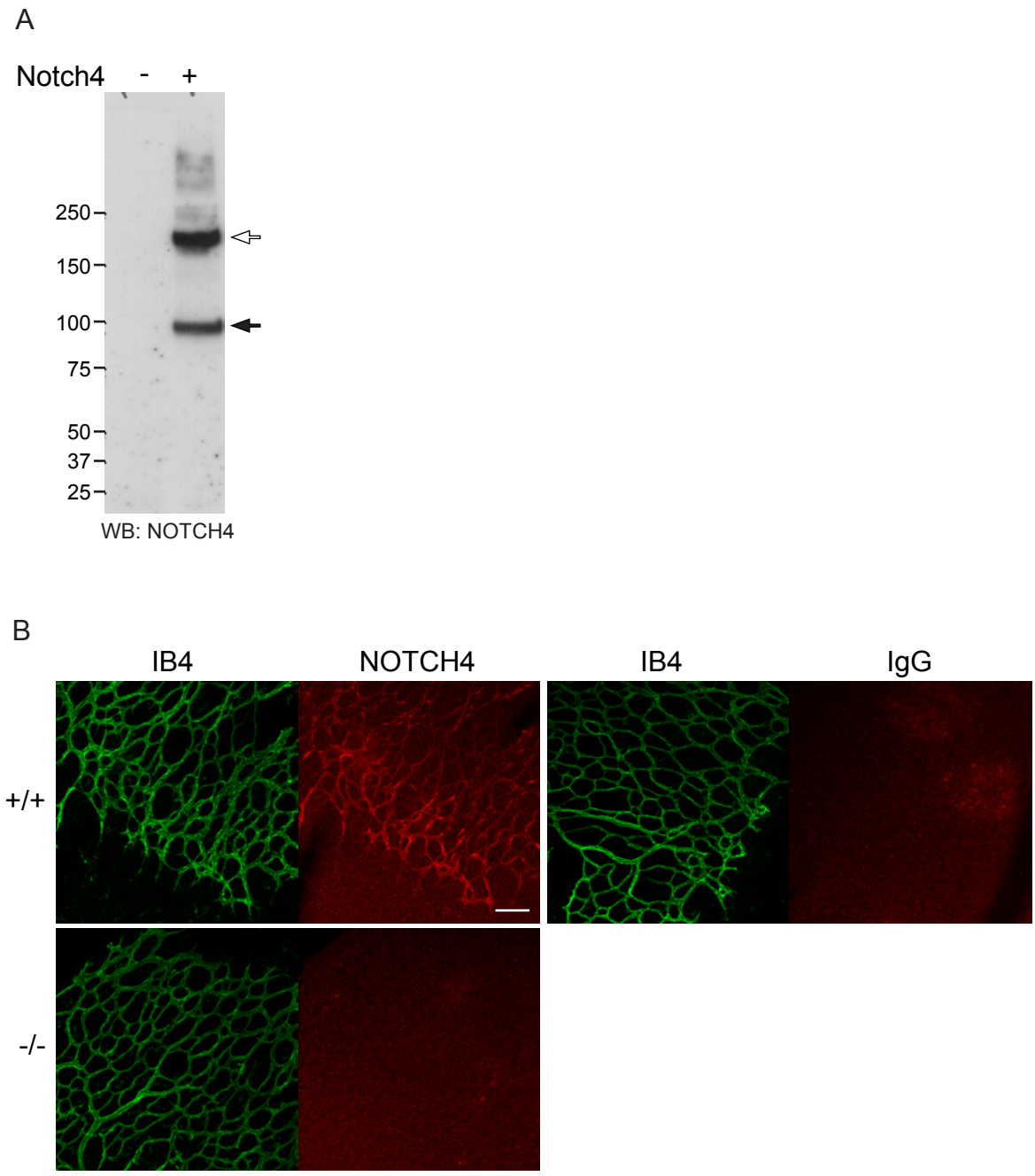

Supplemental Figure 2. Anti-NOTCH4 extracellular domain (EC) antibody specifically detects NOTCH4.
(A) The anti-NOTCH4 EC antibody detects full-length (200 kDa; white arrow) and S1-processed NOTCH4 EC domain (100 kDa; black arrow) in NOTCH4-transfected cell lysates but not in untransfected cells. Samples were run on a non-reducing Nu-PAGE gel (Life Technologies) without prior heating to preserve antigen recognition (B) Wholemount detection of anti-NOTCH4 EC reactivity (red) in the vasculature of wildtype (+/+) but not in *Notch4*$^{-/-}$ (-/-) retinas at P5. Vasculature was labelled with Alexa-488 conjugated Isolectin B4 (IB4; green). No staining was evident when an armenian hamster isotype control antibody was applied to wildtype retinas (IgG). The levels of all images were uniformly adjusted to 150 using Photoshop. Scale bar: 100 µm.

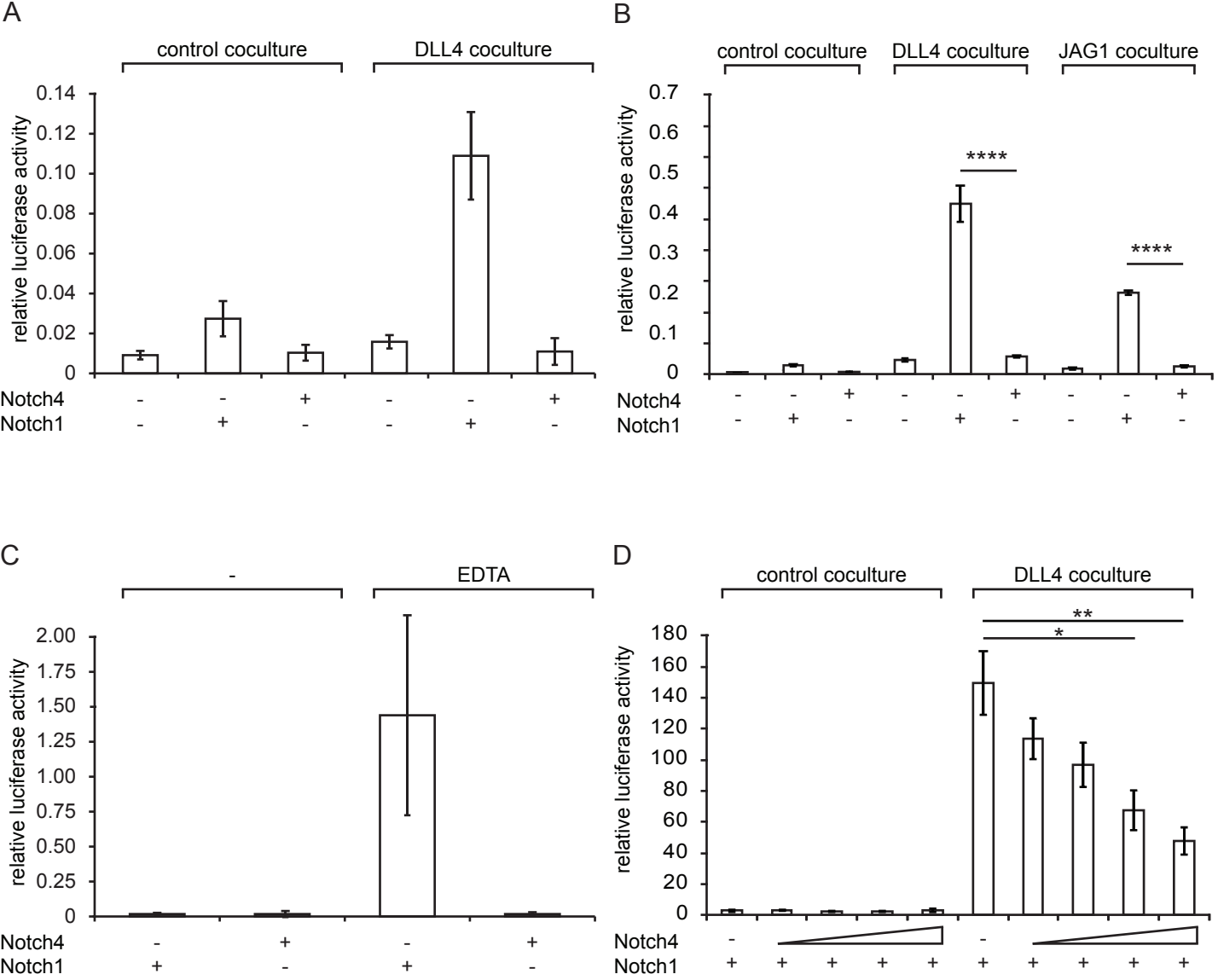

Supplemental Figure 3. NOTCH4 does not signal under a variety of conditions.
(A) Ligand-induced signalling via NOTCH4 and NOTCH1 in the endothelial cell line MAEC. Notch4 or Notch1 cDNA constructs were transiently transfected into MAEC cells along with the Notch responsive reporter and then cocultured with control cells or cells expressing DLL4. (B) Ligand-induced signalling via NOTCH4 and NOTCH1 in the C2C12 cell line. Notch4 or Notch1 cDNA constructs were transiently transfected into C2C12 cells along with the Notch responsive reporter and then cocultured with control cells or cells expressing DLL4 or JAG1. (C) EDTA-induced signalling via NOTCH4 or NOTCH1 in the NIH3T3 cell line. Notch4 or Notch1 cDNA constructs were transiently transfected into NIH3T3 cells along with the Notch responsive reporter and incubated for 5 minutes in PBS containing 0.5 mM EDTA. (D) Ligand-induced signalling via NOTCH1 in the presence of the increasing amounts of NOTCH4 in the NIH3T3 cell line. Notch1 (25 ng/well) and increasing amounts of Notch4 (0, 25, 50, 100 and 200 ng/well) were transiently transfected into NIH3T3 cells along with the Notch responsive reporter and cocultured with control cells or cells expressing DLL4. Signalling is presented as the average relative luciferase activity and standard error of the mean of three independent experiments. These data were tested for statistical significance as described in the experimental procedures. *$p < 0.05$, **$p < 0.01$, ****$p < 0.0001$.

movie 1

Click here to download Supplementary Multimedia File: Movie 1 James et al BBAMCR-14-13R1.mov